

Monte Carlo evaluation of trial wave functions for the fractional quantized Hall effect: Disk geometry

R. Morf

RCA Laboratories Limited, CH-8048 Zurich, Switzerland

B. I. Halperin

Lyman Laboratory of Physics, Harvard University, Cambridge, Massachusetts 02138

(Received 24 June 1985)

Monte Carlo methods have been employed to evaluate the energy of two previously proposed trial wave functions for the quasiparticle at the $\nu = \frac{1}{3}$ quantized Hall state of the two-dimensional electron system. The two wave functions have the same energy within our statistical accuracy, and are consistent with a value $\tilde{\epsilon}_+(\frac{1}{3}) \approx (0.073 \pm 0.008)e^2/\epsilon l_0$, where l_0 is the magnetic length, and ϵ the background dielectric constant. Simulations of the quasihole state confirm previous estimates of $\tilde{\epsilon}_-(\frac{1}{3}) \approx 0.026e^2/\epsilon l_0$. We have also studied the charge distributions of the quasiparticle and quasihole states, and we have evaluated the energies of a previously proposed microscopic trial wave function for the ground state at $\nu = \frac{2}{5}, \frac{2}{3},$ and $\frac{2}{7}$.

I. INTRODUCTION

The fractional quantized Hall effect is characterized by plateaus in the Hall conductance of a two-dimensional electron system, where the Hall conductance is pinned at a rational fraction ν of the fundamental unit e^2/h .¹ Current explanations of this effect require that the ideal two-dimensional electron system, in a uniform positive background, must have a series of stable states at the corresponding filling factors $\nu = N/N_\Phi$ of the first Landau level, where N is the number of electrons, and N_Φ the number of flux quanta in the system.¹⁻⁴ (By a stable state, we mean that there is a positive discontinuity in the derivative $\partial E/\partial N$ of the total energy of the system at the filling factor ν .) In a seminal paper, Laughlin³ proposed an approximate form for the electron wave function at filling factors $\nu = 1/m$, where m is an odd integer, and gave arguments why there should be a discontinuity in $\partial E/\partial \nu$ at these values of ν . Since a collection of electrons in the lowest Landau level has a particle-hole symmetry,⁵ in the limit where the cyclotron frequency is large enough to neglect mixing in of higher Landau levels by the electron-electron interaction, it follows that there should exist analogous stable states at filling factors $\nu = 1 - m^{-1}$.

However, experiments indicating quantized plateaus at filling factors such as $\frac{2}{5}, \frac{2}{7}, \frac{3}{7}, \frac{3}{5},$ and $\frac{4}{5}$ clearly require some nontrivial extension of Laughlin's idea to describe the corresponding stable states.¹

Another key result of Laughlin's paper³ was the observation that the elementary charged excitations in a stable state $\nu = 1/m$ would be quasiparticles and quasiholes with electric charge $\pm e/m$. For more general rational ν , the elementary excitations have charge $\pm qe$, where $|q|^{-1}$ is the denominator of the fraction ν , expressed as a fraction in lowest terms. Since the addition of one electron requires the addition of $|q|^{-1}$ elementary excitations, the discontinuity in slope of the energy curve may be written

$$\left. \frac{\partial E}{\partial N} \right|_{\nu+} - \left. \frac{\partial E}{\partial N} \right|_{\nu-} = \frac{\tilde{\epsilon}_+ + \tilde{\epsilon}_-}{|q|}, \tag{1.1}$$

where $\tilde{\epsilon}_+ + \tilde{\epsilon}_-$ is the energy necessary to create one quasiparticle and one quasihole well separated from each other. (The precise definitions of the individual excitation energies $\tilde{\epsilon}_+$ and $\tilde{\epsilon}_-$ will be discussed in Sec. II D.)

The energy gap $E_g \equiv \tilde{\epsilon}_+ + \tilde{\epsilon}_-$ is also of crucial importance in determining the low-temperature electrical properties of the system. For example, in the limit of small but nonzero impurity concentrations, we expect that the electrical resistance ρ_{xx} will be thermally activated, with an activation energy $E_g/2$. Thus it is of great importance to be able to calculate the excitation energies $\tilde{\epsilon}_+$ and $\tilde{\epsilon}_-$ for any stable ν of experimental interest.

It has been proposed that the quasiparticles or quasiholes of Laughlin's stable states $\nu = 1/m$ can be used as building blocks to describe a set of higher-order stable states, with more general rational values of ν ; for example, the $\nu = \frac{2}{5}$ state was obtained by adding quasiparticles to the state $\nu = \frac{1}{3}$.^{4,6-8} In fact, by hierarchical iteration of the quasiparticle construction, one can build, at least formally, any rational fraction with odd denominator, in the range $0 < \nu < 1$, as was first noted by Haldane.⁶⁻⁸

In a previous paper by one of the authors, it was pointed out that a collection of quasiparticles may be described by a macroscopic *pseudo-wave-function*, which is a function only of the quasiparticle coordinates, and which has a form appropriate for a set of fractionally charged particles obeying fractional statistics, in the lowest kinetic-energy level in the applied magnetic field.⁸ In this way one was led to a set of *estimates* of the ground-state energies at the various stable filling factors ν , which depend in each case on the quasiparticle or quasihole energies at previous levels of the hierarchy. For example, using this approach we may write⁸

$$(E/N)_{\nu=2/5} \approx A + \frac{1}{2} \tilde{\epsilon}_+(\frac{1}{3}), \quad (1.2)$$

where $\tilde{\epsilon}_+(\frac{1}{3})$ is the quasiparticle energy for $\nu=\frac{1}{3}$, the coefficient $\frac{1}{2}$ reflects the fact that the density of quasiparticles is one-half the number of electrons, in the $\frac{2}{5}$ state, and the constant A includes the energy of the parent $\nu=\frac{1}{3}$ state and the energy of interaction of the quasiparticles. The value of A , in this approximation, is derived from the pair-correlation function of a classical one-component plasma, and has the approximate value $A = -0.461$ (see discussion in Appendix A). [Note: All energies in this paper, unless otherwise specified, will be quoted in units of $e^2/\epsilon l_0$, where ϵ is the dielectric constant arising from the polarizability of the bulk semiconductor material, and $l_0 = |\hbar c/eB|^{1/2}$ is the magnetic length. Also, our discussion is confined to the strong magnetic limit $\hbar\omega_c \gg e^2/\epsilon l_0$ with all electrons in the lowest spin state of the lowest Landau level.]

In the present paper we shall present calculations of the quasiparticle energy $\tilde{\epsilon}_+$ at filling factor $\nu=\frac{1}{3}$, and of the total energy E for the stable groundstate at $\nu=\frac{2}{5}$. In each case, these involve a Monte Carlo evaluation of the expectation value of the energy in a *microscopic* trial wave function, which is a specified function of the positions of all the electrons in the system. The trial wave function employed for the state $\nu=\frac{2}{5}$ has the pair form proposed previously by one of us [Eq. (21) of Ref. 4]. For the quasiparticle, we have used two different trial wave functions: the pair form suggested in Eq. (23) of Ref. 4 and the derivative form suggested by Laughlin in Eq. (14) of Ref. 3. [See Eqs. (2.38), (2.18), and (2.17) below.]

Results of our calculations of the quasiparticle energy $\tilde{\epsilon}_+$ at $\nu=\frac{1}{3}$, based on Laughlin's derivative wave function, are shown in Fig. 7 below for systems of up to 72 particles. In particular, for the 72-particle system, we find the result

$$\tilde{\epsilon}_+ = 0.0698 \pm 0.0033. \quad (1.3a)$$

Although there is no clear way of extrapolating our finite-size results to an infinite system, we believe that a reasonable estimate is

$$\tilde{\epsilon}_+ = 0.073 \pm 0.008. \quad (1.3b)$$

Numerical results for $\tilde{\epsilon}_+$ based on the pair-wave-function form are given in the final column of Table II, below, for systems of up to $N=42$ particles. Although the energies obtained appear to be consistently slightly lower than the energies of the Laughlin's derivative wave function at the same values of N , the larger uncertainties of these calculations prevent us from attributing significance to this energy difference.

Although the energy of a trial wave function is necessarily an upper bound to the exact energy of a system containing one quasiparticle excitation in the $\nu=\frac{1}{3}$ state, our quasiparticle energy $\tilde{\epsilon}_+$ is not a rigorous upper bound because it requires subtraction of the ground-state energy at $\nu=\frac{1}{3}$, for which we only have a variational approximation. However, within the spirit of Laughlin's analysis, it seems most likely that the variational energy for the spatially inhomogeneous quasiparticle state should be less ac-

curate than the estimate for the simple $\nu=\frac{1}{3}$ state. Therefore we expect that our result (1.3) will be somewhat larger than the exact value of $\tilde{\epsilon}_+$ in the $\nu=\frac{1}{3}$ state.

We note that all of our results for $\tilde{\epsilon}_+$ at $\nu=\frac{1}{3}$ are significantly higher than the estimate $\tilde{\epsilon}_+ \approx 0.030$ given by Laughlin in Ref. 7, or the estimate $\tilde{\epsilon}_+ \approx 0.025$ obtained recently by Chakraborty.⁹ The estimates of Laughlin and Chakraborty were based on the same trial wave function as we have used to obtain the results (1.3), but involved the use of further approximations to obtain the energy. The present results imply that these further approximations were inaccurate by approximately a factor of 2.

Our result for the energy per particle at $\nu=\frac{2}{5}$ is

$$E/N \approx -0.414 \pm 0.002. \quad (1.4)$$

In addition to the quoted statistical error and the unknown (positive) error due to the inexactness of our trial wave function, there is an error in this case because we have included the effects of antisymmetrization only to second order in the exchange between pairs. However, we estimate the antisymmetrization error, as well as the finite-size effects, to be small.

The result for $\nu=\frac{2}{5}$ is *not* in satisfactory agreement with the result $E/N \approx -0.435$, obtained by Yoshioka, from exact diagonalizations of systems with up to $N=6$ particles, in a rectangular cell with periodic boundary conditions.² Thus, it seems that this proposed form of the microscopic wave function is a rather poor approximation to the true ground state at $\nu=\frac{2}{5}$. In contrast, the estimate obtained via Eq. (1.2), using our calculated value $\tilde{\epsilon}_+(\frac{1}{3}) \approx 0.073$, gives $E/N \approx -0.424$, for the $\nu=\frac{2}{5}$ state, which is much closer to Yoshioka's results.

In Ref. 3 Laughlin proposed a simple trial wave function for the state of one *quasihole*, added to the ground state at $\nu=1/m$, whose energy may be evaluated directly by Monte Carlo methods, or by approximations such as the hypernetted chain. Laughlin quotes the value $\tilde{\epsilon}_- = 0.026$, at $\nu=\frac{1}{3}$, from a modified hypernetted-chain approximation to the pair-correlation function.⁷ We have performed a direct Monte Carlo evaluation of the energy of Laughlin's trial wave function and obtain the results shown in Fig. 4, below, for $N=20, 30, 42$, and 72 particles. Our result for a system of 72 particles is

$$\tilde{\epsilon}_- = 0.0268 \pm 0.0033, \quad (1.5)$$

in good agreement with Laughlin's result. Since the results of Fig. 4 show no change in $\tilde{\epsilon}_-$ from $N=42$ to 72, we regard (1.5) also as our best estimate for $N=\infty$.

If we combine results (1.5) and (1.3a), we obtain a value of the energy gap, for a system of 72 particles, which is

$$E_g \approx 0.0966 \pm 0.0050. \quad (1.6a)$$

Our extrapolation for the energy gap E_g in the infinite system limit is

$$E_g \approx 0.099 \pm 0.009. \quad (1.6b)$$

This result is substantially larger than the estimate $E_g \approx 0.056$ obtained by Laughlin in Ref. 7, but it is somewhat smaller than a recent estimate $E_g \approx 0.11$ given by

Girvin, MacDonald, and Platzman.¹⁰ The result (1.6) may also be compared with an estimate by Haldane and Rezayi¹¹ of $E_g \approx 0.105 \pm 0.005$ based on computations of the exact energy spectrum of seven electrons on a sphere. We remark that in our disk geometry we expect that finite-size corrections to E_g may be smaller than the separate corrections to $\tilde{\epsilon}_+$ and $\tilde{\epsilon}_-$ because corrections proportional to $N^{-1/2}$ should be equal and opposite for the two terms.

It is interesting to note that experimental values of E_g , extracted from the thermal activation of the electrical resistance at the center of a quantized Hall plateau, have been consistently $\leq 0.03e^2/\epsilon l_0$,¹² significantly smaller than any of the theoretical calculations. The precise reason for this discrepancy is not currently understood.

In the course of our calculations of $\tilde{\epsilon}_+$ and $\tilde{\epsilon}_-$, we had the opportunity also to perform an accurate Monte Carlo evaluation of the energy of the fundamental state at $\nu = \frac{1}{3}$, based on Laughlin's trial wave function. Our result,

$$E/N = -0.410 \pm 0.001, \quad (1.7)$$

is in agreement with the earlier simulations of Levesque, Weis, and MacDonald¹³ for the same trial wave function, and is slightly higher than the exact results of Yoshioka *et al.* for small finite systems.²

Recently, Chui, Hakim, and Ma¹⁴ have carried out a simulation for a crystal-like trial wave function for the $\nu = \frac{1}{3}$ state, which they report has a significantly lower energy than that of Laughlin's wave function quoted above. Indications of a crystal-like pair-correlation function have also been found in a renormalization-group analysis by Chui.¹⁵ In the present paper, however, we shall adhere to the "conventional" view, namely that the Laughlin trial function is a good physical approximation to the true ground state at $\nu = \frac{1}{3}$.

The remainder of this paper describes our calculations in some detail. In Sec. II, we discuss the forms of the trial wave functions used in the calculations, along with some of the motivation for the choices. The energies $\tilde{\epsilon}_+$ and $\tilde{\epsilon}_-$ are also defined in this section.

The methods used to evaluate the energies of our trial wave functions are discussed in Sec. III. Detailed numerical results for the energies are also presented in this section, and we also discuss the charge-density distribution in the case of the quasiparticle state. Also included are results of simulations for the $\nu = \frac{2}{7}$ and $\frac{2}{3}$ states, based on trial wave functions that are closely related to the one used for $\nu = \frac{2}{5}$.

The arguments leading to the approximate energy formula (1.2) are briefly discussed in Appendix A. Some computational strategies, employed to permit efficient implementation of our program on an array processor, are discussed in Appendix B.

All simulations in the present paper have been carried out in a planar disk geometry, with particle numbers ranging from $N=20$, up to a high $N=196$ for certain portions of the analysis. Generalizations to a spherical geometry are currently being studied. We note that the wave functions for the quasiparticle at $\nu = \frac{1}{3}$ can be readily adopted to a spherical geometry, but the trial wave

function for the $\nu = \frac{2}{5}$ state has required physically significant modification to permit implementation on the sphere. Details of these generalizations will be presented elsewhere.

II. FORM OF THE TRIAL WAVE FUNCTIONS

A. The quantum Hall state at $\nu = 1/m$

In this section we present the form of the trial wave functions used in our calculation, and we review some of the motivation behind these choices.

In all cases we shall confine ourselves to the strong-field limit, where all electrons are restricted to the lowest Landau level.¹⁶ Then we will always have a wave function which is the product of a Gaussian factor $e^{-|r_j|^2/4l_0^2}$ for each electron, and a polynomial in the complex-coordiante variables of the electrons:

$$z_j = x_j - iy_j. \quad (2.1)$$

The form proposed by Laughlin for the fundamental fractional quantized Hall states, having filling factor $\nu = 1/m$, with m odd, is given by

$$\psi_m \equiv \left[\prod_{\substack{i,j=1 \\ i < j}}^N (z_i - z_j)^m \right] \prod_{j=1}^N e^{-|z_j|^2/4l_0^2}. \quad (2.2)$$

This wave function satisfies Pauli statistics, and it has the desirable property that for $m > 1$ the wave function vanishes as a high power of the separation between two electrons, which therefore tends to minimize the repulsive potential energy. The probability distribution of the electrons in the wave function ψ_m is given by

$$|\psi_m|^2 = e^{-H_m}, \quad (2.3)$$

where

$$H_m = -2m \sum_{i < j} \ln |r_i - r_j| + \sum_j \frac{|r_j|^2}{2l_0^2}. \quad (2.4)$$

(Note: Throughout this paper, we shall use probability distributions and wave functions that are not normalized to unity. We define expectation values by $\langle A \rangle \equiv \langle \psi | A | \psi \rangle / \langle \psi | \psi \rangle$.)

Equation (2.4) is the Hamiltonian of a classical one-component plasma of particles interacting with each other and with a uniform neutralizing background via a two-dimensional Coulomb (i.e., logarithmic) interaction. The strong tendency of the plasma to achieve charge neutrality causes the N particles to spread out uniformly in a disk with particle density $\bar{n} = (2\pi m l_0^2)^{-1}$ corresponding to a filling factor $\nu = 1/m$.

The classical Hamiltonian H_m should not be confused with the true quantum-mechanical Hamiltonian H , obeyed by the electrons. The latter is the sum of a kinetic-energy operator T , for N electrons in a uniform magnetic field, and a potential-energy operator V , given by

$$V \equiv \frac{e^2}{2\epsilon} \int \int d^2r \int d^2r' \frac{\rho(\mathbf{r})\rho(\mathbf{r}')}{|\mathbf{r} - \mathbf{r}'|}, \quad (2.5)$$

where the integrals range over the entire x - y plane with the points $\mathbf{r}=\mathbf{r}'$ omitted, and $\rho(\mathbf{r})$ is defined by

$$\rho(\mathbf{r}) \equiv n(\mathbf{r}) - n_b(\mathbf{r}), \quad (2.6)$$

where $n(\mathbf{r})$ is the two-dimensional electron-density operator, and $-en_b(\mathbf{r})$ is the charge density of the neutralizing uniform positive background sheet. Note that V involves the *three-dimensional* Coulomb interaction, $\propto 1/r$, in contrast to the logarithmic interaction appearing in the fictitious classical Hamiltonian H_m .

The expectation value of the potential energy in a quantum state ψ is determined by the pair distribution function for the state. In the limit of an infinite system, we have

$$\frac{\langle V \rangle}{N} = \frac{\bar{n}e^2}{2\epsilon} \int_{0^+}^{\infty} dr 2\pi[g(r) - 1], \quad (2.7)$$

where

$$g(r) \equiv \langle n(\mathbf{r})n(\mathbf{0}) \rangle / \bar{n}^2. \quad (2.8)$$

For Laughlin's wave function, we may simply replace $g(r)$ by $g_{p_1}(r)$, the pair-correlation function of the one-component plasma. This function, in turn, may be evaluated to any degree of accuracy, in principle, by molecular-dynamics simulations, or it may be approximated by various standard methods. (Note: The kinetic energy per electron is a constant $\hbar\omega_c/2$ which we shall always omit from our discussion. For this reason, below, we shall often replace $\langle V \rangle$ by the symbol E , for energy.)

It is convenient, for our purposes, to discuss the energy of a finite system. For this we consider that the positive charge which neutralizes the electrons is spread uniformly over a disk of radius R_m , with

$$\pi R_m^2 = 2\pi m l_0^2 N. \quad (2.9)$$

The potential energy of the system is then given by

$$E = \frac{e^2}{2\epsilon} \int' d^2r \int d^2r' \frac{\langle \rho(\mathbf{r})\rho(\mathbf{r}') \rangle}{|\mathbf{r}-\mathbf{r}'|}, \quad (2.10)$$

where the integrations run from $r=0$ to $r=\infty$, with the points $\mathbf{r}=\mathbf{r}'$ excluded, and

$$\rho(\mathbf{r}) = \begin{cases} n(\mathbf{r}) - \bar{n} & \text{for } 0 \leq r \leq R_m, \\ n(\mathbf{r}) & \text{for } r > R_m. \end{cases} \quad (2.11)$$

The expectation value $\langle \rangle$ is to be evaluated in this case using the probability density (2.3), for a finite system of N electrons. Note that the average electron density $\langle n(\mathbf{r}) \rangle$ does not drop off sharply to zero at $r=R_m$, but rather spills out slightly, falling off with a length scale of order l_0 about $r=R_m$.

B. The quasihole state

An important characteristic of Laughlin's wave function (2.2) is the number and location of the zeroes of the function. If all electrons but one are held fixed, and the wave function considered to be a function of the position z_j of the remaining electron, then we see that there are precisely m zeroes at the position of each fixed electron, z_k . Equivalently, we note that the phase of the wave function changes by $2\pi m N'$ if the "test-electron" position

z_j is moved around a path encircling N' other electrons. As stated above, in the strong-field limit, we consider only wave functions which are a product of a Gaussian factor and a polynomial in complex position coordinates $\{z_i\}$. The properties of analytic functions are such that if the magnitude of ψ is to remain approximately constant over a large region, the average density of zeroes of the wave function must not deviate from the value $1/2\pi l_0^2$. Since Laughlin's wave function has m zeroes per electron, this fixes the density at $\nu=1/m$.

In order to have a density of electrons slightly *smaller* than $\nu=1/m$, it is necessary to have some extra zeroes of the wave function with no electrons attached, or else to have some electrons with more than m zeroes. The first possibility is easiest to realize. Consider the wave function

$$\psi_\eta^{(-)}[z_i] = \prod_{j=1}^N (z_j - \eta) \psi_m[z_j], \quad (2.12)$$

with $\eta = \eta_x - i\eta_y$ and $|\eta| < R_m$.

This wave function has a simple zero at $z_j = \eta$ for any j , as well an m -fold zero at each point where $z_j = z_k$, for $k \neq j$. Since the zeroes must be uniformly spread out with a density equal to the density of flux quanta, this suggests that there will be a hole in the electron distribution in the vicinity of point η , with $1/m$ electrons missing, and that the radius of the disk occupied by the electrons will increase slightly to accommodate the extra $1/m$ electron. Indeed, if we consider the square of the wave function $\psi_\eta^{(-)}$, we find

$$|\psi_\eta^{(-)}[z_j]|^2 = e^{-H_\eta^{(-)}}, \quad (2.13)$$

where

$$H_\eta^{(-)} = H_m + 2 \sum_j \ln |z_j - \eta|. \quad (2.14)$$

This is just the Hamiltonian of a classical one-component plasma in the presence of an extra repulsive "ghost charge," at point η , whose strength is smaller by a factor $1/m$ than the charges in the plasma. The tendency of the plasma to establish charge neutrality guarantees that the ghost charge will be "screened" by a deficit of $1/m$ electrons in the vicinity of the point η , while the electron density elsewhere in the interior of the occupied disk is the same as in the absence of the ghost charge. Of course, if the number N of electrons is held fixed, the radius of the occupied disk must expand slightly (by a fraction $\approx 1/2mN$), in order to accommodate the ghost charge as well as the electrons.

Recall that the real three-dimensional electric charge is carried by the electrons and by the uniform positive background, not by the fictitious ghost charge. Since the electron charge density just cancels the uniform background in the absence of the ghost charge, it is clear there is a real net charge of positive sign in the vicinity of point η , whose value is just $-1/m$ times the electron charge e . This charge is concentrated in a radius $\approx l_0$ about the point η .

The quasihole wave function (2.12) is not an exact eigenstate of the Hamiltonian. It is certainly the simplest

wave function, however, that has the necessary property of enclosing one extra flux quantum, and it is very much in the same spirit as the ground-state trial wave function (2.2). Therefore, if (2.2) is a good approximation to the true ground state of the uniform system, it seems likely that (2.12) will be a good approximation to the lowest-energy state containing one extra zero in the interior. We may note that both (2.2) and (2.12) are exact energy states in the limit of a short-range potential.¹⁷

C. The quasiparticle state

In order to increase the density of electrons relative to the stable $1/m$ value, we must create a state in which there is slightly less than m flux quanta per electron in the interior of the system. Thus we seek a quasiparticle state, in which there is one missing flux quantum, or one missing zero of the wave function, relative to the state (2.2). In this case the choice of trial wave function is less obvious than in the case of a quasihole. We cannot simply multiply the wave function (2.2) by $\prod_j (z_j - \eta)^{-1}$, because the resulting wave function would no longer be of the form of an analytic function of z times a Gaussian function, and thus would not describe particles in the first Landau level.

If we did not have to worry about antisymmetrization of the wave function, we could consider a trial wave function of the form

$$\psi = \prod_{j=2}^N (z_j - z_1)^{-1} \psi_m, \quad (2.15)$$

in which electron 1 is distinguished from all others. This wave function is nonsingular, because ψ_m vanishes when $z_j \rightarrow z_1$. $|\psi|^2$ is the distribution function for a two-dimensional plasma in which particle 1 has its charge reduced by the factor $(m-1)/m$ in its repulsive interaction with the other particles, but has the same interaction as the other particles in its attractive interaction with the background. It is clear that particle 1 will be attracted to the center of the occupied disk, and the remaining electrons will leave a hole near the origin of size $(m-1)/m$. The net effect is an extra negative charge e/m near the origin. Alternatively, we may note that when (2.15) is considered to be a function of the position of any electron other than the singled-out electron 1, there is one less zero of the wave function than in the case of the ground state ψ_m .

Equation (2.15) is actually a valid trial wave function for a quasiparticle excitation in which the spin of one electron is reversed relative to spins of all the others, since electrons of spin up and spin down may be treated as two distinguishable species. The potential energy of (2.15) should be only slightly higher than the energy of the ground state (2.2); although the singled-out electron does approach its neighbors somewhat more closely than in the ground state, $|\psi|^2$ still vanishes as $|z_j - z_1|^{2m-2}$. Indeed, the potential-energy cost of this excitation is probably lower than that of any other simple quasiparticle wave function, and it is only the *Zeeman energy* associated with the spin reversal that we believe will suppress this excitation in most practical cases.¹⁸ [In the limit of

short-range repulsive interactions, Eq. (2.15) should actually become an exact eigenstate for a spin-reversed quasiparticle excitation, and should be the lowest-energy quasiparticle in the absence of the Zeeman energy.]

If all electrons are assumed to have parallel spins, then Eq. (2.15) is an illegal trial function, as it is not antisymmetric under interchange of particle 1 with the other particles. We might attempt to repair this difficulty by operating on the wave function with the antisymmetrizer α , defined by

$$\alpha \equiv \sum (-1)^{[P]} P, \quad (2.16)$$

where the sum is over all permutations P of the positions z_j , and $(-1)^{[P]}$ is the sign of the permutation. It can be shown, however, that the antisymmetrizer annihilates the wave function (2.15). Specifically, we note that if we consider the dependence of $\alpha\psi$ on one of its variables, say z_j , while all the others are held fixed, then it has the form of the product of the fundamental ground state ψ_m and a rational function $R(z_j)$ which goes to zero for $z_j \rightarrow 0$ and which has only simple poles, occurring at the points $z_j = z_k$, for $k \neq j$. Since $\alpha\psi$ is odd under interchange of z_j and z_k , however, it follows that it must vanish as an odd power of $z_j - z_k$, when the two points come together. This implies the residue at the poles of $R(z_j)$ are equal to zero, and hence $R(z_j) \equiv 0$.

A properly antisymmetrized trial wave function for a (spin-aligned) quasiparticle state at point $z = \eta$ has been proposed by Laughlin.³ It may be written

$$\psi = \prod_{j=1}^N \left[e^{-|z_j|^2/4l_0^2} \left(2l_0^2 \frac{\partial}{\partial z_j} - \eta^* \right) \right] \prod_{l < k} (z_l - z_k)^m. \quad (2.17)$$

Although the square of this wave function cannot be directly interpreted as the distribution function of a classical statistical-mechanics problem, Laughlin has shown that the charge density can be calculated using a mathematical transformation. Indeed, the wave function has the requisite properties of a quasiparticle state: the charge density is the same as for the ground state ψ_m , except within a radius of order l_0 about $z = \eta$, where one finds a total extra charge of e/m . One may also verify by inspection of (2.17) that it has one missing zero as a function of any variable z_j , compared to ψ_m . We refer the reader to Refs. 3 and 7 for further justification of this trial wave function.

In addition to employing the wave function (2.17), we have used an alternate trial wave function, suggested earlier by one of us,⁴ which appears to be more directly motivated by a classical statistical-mechanics problem. We write our wave function, for the case of a quasiparticle at the origin, as

$$\psi_0^{(+)}\{z_k\} = \alpha \tilde{\psi}_0^{(+)}\{z_k\}, \quad (2.18a)$$

$$\tilde{\psi}_0^{(+)}\{z_k\} = \left[\frac{1}{z_1 - z_2} \right]^2 \prod_{j=3}^N \frac{z_j - \frac{1}{2}(z_1 + z_2)}{(z_1 - z_j)(z_2 - z_j)} \psi_m. \quad (2.18b)$$

Let us first ignore the antisymmetrizer and examine the properties of the wave function $\tilde{\psi}_0^{(+)}$. We note that $\tilde{\psi}_0^{(+)}$

has the form of a polynomial in $\{z_k\}$, times a Gaussian factor, and hence describes a collection of particles in the lowest Landau level, as long as we have $m > 1$. The square of the wave function may be written

$$|\tilde{\psi}_0^{(+)}|^2 = e^{-\tilde{H}}, \quad (2.19)$$

$$\begin{aligned} \tilde{H} = & H_m + 4 \ln |\mathbf{r}_1 - \mathbf{r}_2| \\ & + 2 \sum \left[\ln |\mathbf{r}_j - \mathbf{r}_1| + \ln |\mathbf{r}_j - \mathbf{r}_2| \right. \\ & \left. - \ln \left| \mathbf{r}_j - \frac{\mathbf{r}_1 + \mathbf{r}_2}{2} \right| \right], \end{aligned} \quad (2.20)$$

where H_m is the Hamiltonian of the classical one-component plasma (2.4). Thus, compared with H_m , we see that \tilde{H} has an extra logarithmic attraction between particles 1 and 2, which tends to keep them bound together. The remaining particles have a logarithmic repulsive interaction with the center of gravity of the bound pair, in addition to a logarithmic attraction to the two members of the pair, which partially cancels the repulsion contained in H_m . The net effect is that an electron which is some distance away from the pair sees a net charge on the pair of $2m - 1$, in units where an unpaired electron has charge m . There will therefore be a hole of size $2 - 1/m$ about the pair, i.e., including the pair, there will be a net charge of e/m .

Just as in the wave function (2.15), the extra negative charge will be attracted to the center of the system. The pair sees an effective repulsive potential energy, arising from the interaction with the uniform density of other electrons, which has the form $-(2 - m^{-1})r^2/2l_0^2$, but the interaction of the two particles with the uniform background gives a larger attractive potential r^2/l_0^2 . The net effect is an attraction of $r^2/2ml_0^2$, which localizes the pair at the origin. A similar analysis also shows that the interactions between the singled-out pair and the remaining electrons lead to an effective quadratic attraction between the two particles of the pair, which tends to enhance the binding of the pair.

The above analysis can be generalized to a state in which the quasiparticle charge is centered at a point η rather than at the origin. We define

$$\psi_\eta^{(+)} = \alpha \tilde{\psi}_\eta^{(+)}, \quad (2.21)$$

$$\tilde{\psi}_\eta^{(+)} = e^{\eta^*(z_1+z_2)/4ml_0^2} \tilde{\psi}_0^{(+)}. \quad (2.22)$$

If we set $z_1 \approx z_2 \approx z$, and integrate over the positions of the remaining electrons, then the value of $|\tilde{\psi}_\eta^{(+)}|^2$ is proportional to $\exp[-V^{\text{eff}}(z)]$, where

$$V^{\text{eff}} = (-2 \text{Re} \eta^* z + |z|^2)/2ml_0^2. \quad (2.23)$$

Thus $|\tilde{\psi}_\eta^{(+)}|^2$ has its maximum when the center of gravity of the singled-out pair is at the point $z = \eta$.

Next, we would like to argue that the unsymmetrized wave function $\tilde{\psi}_0^{(+)}$ has a reasonably low expectation value of the potential energy V , and from that point of view is a good starting point for the desired wave function

of a quasiparticle at the origin. We see, of course, that for most pairs of electrons the correlations are the same as in the uniform ground state ψ_m . The pair z_1 and z_2 approach each other more closely than the others, as $|\tilde{\psi}_0^{(+)}|$ is seen to vanish only as $|z_1 - z_2|^{m-2}$, and this will certainly increase the energy somewhat. This feature must be characteristic of *any* antisymmetrized wave function which has a higher density of electrons than present in the state ψ_m , however, so we must be prepared to pay such an energy price. Now, consider the interaction of the electron 1 with the remaining electrons in the system. The wave function $|\tilde{\psi}_\eta^{(+)}|$ vanishes only as $|z_1 - z_j|^{m-1}$, which is slightly slower than in the original wave function ψ_m . However, the electron j is repelled from the electron 2 and from the center of gravity of the pair 1 and 2 by additional terms in the classical Hamiltonian \tilde{H} , while electron 1 is closer to electron 2 than it would be to its nearest neighbor in ψ_m . Thus the distance between electron 1 and any electron other than 2 is probably slightly greater than it would be in the state ψ_m . This should reduce the energy somewhat.

Finally, we must examine the effects of the antisymmetrizer α . We note that the wave function $\tilde{\psi}_0^{(+)}$ is already antisymmetric with respect to the interchange of particles j and k , if $j > 2$ and $k > 2$, and it is also antisymmetric under interchange of particles 1 and 2. However, the wave function does not simply change sign under a permutation such as P_{13} which interchanges the positions of particle 1 and particle 3. If the pair 1 and 2 were very tightly bound, and had no overlap in space with the region occupied by particle 3, then the function $P_{13}\tilde{\psi}_0^{(+)}$ would have no overlap with the original function $\tilde{\psi}_0^{(+)}$. There would then be no contribution of the cross term $\langle \tilde{\psi}_0^{(+)} | P_{13} \tilde{\psi}_0^{(+)} \rangle$ to the normalization of the wave function $\psi_0^{(+)}$, and no contribution of $\langle \tilde{\psi}_0^{(+)} | V | P_{13} \tilde{\psi}_0^{(+)} \rangle$ to the expectation value of the potential energy.

Since $P_{13}^2 = 1$, and P_{13} commutes with V , the terms

$$\langle \tilde{\psi}_0^{(+)} | P_{13} V P_{13} | \tilde{\psi}_0^{(+)} \rangle \quad \text{and} \quad \langle \tilde{\psi}_0^{(+)} | P_{13} P_{13} | \tilde{\psi}_0^{(+)} \rangle,$$

which appear in the numerator and denominator of the expectation value are equal to, respectively,

$$\langle \tilde{\psi}_0^{(+)} | V | \tilde{\psi}_0^{(+)} \rangle \quad \text{and} \quad \langle \tilde{\psi}_0^{(+)} | \tilde{\psi}_0^{(+)} \rangle,$$

and have no effect on the ratio.

In actual practice we do not expect there to be zero overlap of the pair (z_1, z_2) with the other electrons in the system, but we may hope that the overlap is sufficiently small that the antisymmetrizer α has only a modest effect on the energy and correlation functions for the quasiparticle state. In the Monte Carlo calculations described below, where we have taken the antisymmetrizer fully into account, we find that these expectations are reasonably fulfilled. The antisymmetrization process actually leads to a reduction in the quasiparticle energy $\tilde{\epsilon}_+$ by about 40%, at $\nu = \frac{1}{3}$.

It should be noted that we have no strong *a priori* reason to believe that our quasiparticle wave function (2.18) is any better or any worse than Laughlin's trial wave function (2.17). It turns out that the energies of the two wave functions are very similar, although there are

some differences in the charge distribution, as discussed in Sec. III.

To see the possible similarity between the two trial wave functions, note that if we set $\eta=0$ in Eq. (2.17), and consider a particular *subset* of the many terms which result from allowing the derivatives to act on different factors in the polynomial $\prod_{l < k} (z_l - z_k)^m$, we can recover our own antisymmetrized wave function (2.18). In particular, if we let $\partial/\partial z_1$ and $\partial/\partial z_2$ act on the factor $(z_1 - z_2)^m$, and we let $\partial/\partial z_k$ act on the factor $(z_1 - z_k)^m(z_2 - z_k)^m$, for all $k \geq 3$, we just recover the unsymmetrized wave function $\psi_0^{(+)}$; if we include all the permutations of this term, we obtain the antisymmetrized form $\psi_0^{(+)}$. It is not *a priori* clear whether the remaining omitted terms should increase or decrease the energy of the state, nor is it clear that the omitted terms lead to any large differences in the properties of the two wave functions.

D. Definition of the quasiparticle energy

Having chosen a particular trial wave function $\psi_0^{(+)}$ or $\psi_0^{(-)}$ for the state with quasiparticle or quasihole at the origin, we may, in principle, calculate the expectation value of V , and so determine the energy of the state. To identify the quasiparticle or quasihole energy, however, we must subtract off the energy of the stable ground state ψ_m , and here an ambiguity arises: Should we choose ψ_m at the same value of magnetic field or the same electron-disk radius? Should we consider a system with same number of electrons, or should we alter the total number of electrons by $\pm 1/m$, consistent with the idea that the quasiparticle and quasihole carry an electric charge $\pm e/m$? One may also question whether to alter the radius of the neutralizing background by an amount of order $1/2mN$.

Following Ref. 8, we shall give here two distinct definitions of the quasiparticle energy. A "gross" energy ε_+ of the quasiparticle may be defined by the following *Gedanken* experiment. We begin with a Laughlin state $\nu=1/m$, containing N electrons in a uniform magnetic field B_0 , interacting with a uniform positive background of charge $-Ne$, spread over a disk of area $\pi R_m^2 = 2\pi N m l_0^2$. Let the energy of this state be E_m . Now let us add one electron to the system, together with a neutralizing background charge of $-e$, which is spread uniformly over the disk of radius R_m . We hold the magnetic field constant and we require that the extra electron goes into the system in the form of m quasiparticles of charge e/m , well separated from each other in space, and also far from the boundaries of the system. Note that the outer radius of the disk occupied by the $N+1$ electrons will be the same as that occupied by the N electrons in the original state, and the electron density is unchanged, except near the quasiparticles. Now we define the quasiparticle energy ε_+ as $1/m$ times the energy difference between the new state and the original energy E_m . Note that ε_+ is defined so that in the limit of an infinite system, it is precisely equal to $m^{-1} \partial E / \partial N$, where E is the total potential energy, and the derivative is evaluated at fixed magnetic field, in the limit $\nu \rightarrow (1/m)^+$.

In Ref. 8 we also defined a "proper" quasiparticle energy $\tilde{\varepsilon}_+$. For the case of a quasiparticle added to one of the fundamental fractional Hall states with $\nu=1/m$, the proper energy may be defined as follows.¹⁹ Again, we begin with a state ψ_m containing N electrons in a field B_0 . Now, however, we keep the number of electrons constant and reduce the magnetic field by a factor $mN/(mN+1)$. We require that the new electron states have one quasiparticle at the origin, i.e., we have a state similar to $\psi_0^{(+)}$ of Eq. (2.18). Since the magnetic length which enters the wave function has been increased by the factor $|(mN+1)/mN|^{1/2}$, we find that the outer radius of the occupied electron disk is the same as in the original state ψ_m ; the extra charge e/m at the origin is compensated by a reduction in the uniform electron density elsewhere in the disk, which is in proportion to the reduction in B . The proper quasiparticle energy $\tilde{\varepsilon}_+$ is then defined as the difference in the potential energy of the present state and the original starting state ψ_m . We may thus describe $\tilde{\varepsilon}_+$ as the change in potential energy upon removing one quantum of magnetic flux from the system at $\nu=1/m$.

In precise analogy to the above constructions, we define a gross energy ε_- and a proper energy $\tilde{\varepsilon}_-$ for adding a quasihole to the fundamental state at $\nu=1/m$.

It is not difficult to find the relation between ε_+ and $\tilde{\varepsilon}_+$ in the limit of large N .⁸ Consider a fundamental quantum Hall state at filling factor $\nu=1/m$, which contains $N+1$ electrons in a magnetic field $B_0(N+1)/N$. Since the potential energy per electron of a given state is inversely proportional to the magnetic length l_0 , the total potential energy of the state under discussion may be written as

$$\left(\frac{N+1}{N} \right)^{3/2} E_m \approx \left[1 + \frac{3}{2N} \right] E_m, \quad (2.24)$$

where E_m is the energy of the state with N electrons in field B_0 , as before.

Now if we repeat m times the construction used to define the proper energy $\tilde{\varepsilon}_+$, beginning with the state with $N+1$ particles, locating the quasiparticle at a different point each time as we reduce the field by the factor $Nm/(Nm+1)$, we wind up with a state containing $N+1$ particles in a field B_0 , which is precisely the state we used above to define the gross energy ε_+ .

It follows that

$$\varepsilon_+ = \tilde{\varepsilon}_+ + \frac{3}{2m} \frac{E_m}{N}. \quad (2.25)$$

In a similar way, we find, for the quasihole energies,

$$\varepsilon_- = \tilde{\varepsilon}_- - \frac{3}{2m} \frac{E_m}{N}. \quad (2.26)$$

Note that for quantities such as the energy gap E_g which involve the sum of the quasiparticle and quasihole energies, it does not matter whether we use the proper energies or the gross energies, since

$$\varepsilon_+ + \varepsilon_- = \tilde{\varepsilon}_+ + \tilde{\varepsilon}_-. \quad (2.27)$$

The difference between the individual energies is not

small, however. For example, in the case $m=3$ ($\nu=\frac{1}{3}$) we have $E_m/N \approx -0.410e^2/\epsilon l_0$. Then the values $\tilde{\epsilon}_+ \approx 0.073e^2/\epsilon l_0$ and $\tilde{\epsilon}_- \approx 0.026e^2/\epsilon l_0$ quoted in the Introduction correspond to gross energies $\epsilon_+ \approx -0.132e^2/\epsilon l_0$ and $\epsilon_- \approx 0.231e^2/\epsilon l_0$.

The quasiparticle and quasihole energies discussed in the remainder of this paper, as in the Introduction, will always be the proper energies $\tilde{\epsilon}_+$ and $\tilde{\epsilon}_-$. The definitions used by Laughlin also coincide with this choice.

E. Finite density of quasiparticles

We now consider the possible states that result from adding a finite density of quasiparticles to a fundamental

state with $\nu=1/m$. If the density of quasiparticles is sufficiently small, we expect that the lowest-energy state should have the quasiparticles localized at the sites of a triangular lattice, forming a Wigner crystal, stabilized by the Coulomb repulsion of the quasiparticles.^{4,20} If the density of quasiparticles is increased sufficiently, however, we expect the Wigner crystal to be unstable to a liquidlike state of the quasiparticles, analogous to the Laughlin states for the bare electrons. It is therefore useful to generalize our quasiparticle wave function to a state with a number of quasiparticles, which need not be in localized positions. We consider a wave function containing N electrons with N_1 quasiparticles. We shall represent these quasiparticles by N_1 pairs of electrons, leaving $N-2N_1$ electrons unpaired. We write

$$\psi\{z_k\} = \alpha \tilde{\psi}\{z_k\}, \quad (2.28)$$

$$\begin{aligned} \tilde{\psi}\{z_k\} \equiv \psi_m\{z_k\} P\{Z_i\} \prod_i (z_{2i} - z_{2i-1})^{-2} \prod_{i < j} [(z_{2i} - z_{2j})(z_{2i-1} - z_{2j})(z_{2i} - z_{2j-1})(z_{2i-1} - z_{2j-1})]^{-1} \\ \times \prod_{i, \gamma} [(Z_i - z_\gamma)(z_{2i} - z_\gamma)^{-1}(z_{2i-1} - z_\gamma)^{-1}], \end{aligned} \quad (2.29)$$

where the index k runs from 1 to N , the indices i and j label pairs and run from 1 to N_1 , the index γ labels unpaired electrons and runs from $2N_1+1$ to N , the variable Z_i is the center of gravity of the i th pair,

$$Z_i = \frac{1}{2}(z_{2i} + z_{2i-1}), \quad (2.30)$$

ψ_m is the Laughlin wave function (2.2), and P is any symmetric polynomial that vanishes at least as fast as $(Z_i - Z_j)^2$ when any pair of variables Z_i and Z_j approach each other. This wave function represents a set of electrons in the lowest Landau level, provided that $m > 1$. The wave function $\tilde{\psi}$ is antisymmetric with respect to the interchange of two unpaired electrons. It is symmetric, as required, with respect to the interchange of two pairs of electrons. It is not yet antisymmetric with respect to interchange of two electrons from different pairs, or interchange of an unpaired electron with a member of a pair. As in the case of a single pair, however, we expect that the properties of $\tilde{\psi}$ will not be drastically altered by the antisymmetrizer, and that we can get good insight by studying the properties of $\tilde{\psi}$.

We can further simplify the problem if we ignore the dependence on the internal degrees of freedom of the pairs. We then write $\psi\{z_k\} \propto \tilde{\phi}\{Z_i, z_\gamma\}$, where

$$\tilde{\phi} \equiv P\{Z_i\} \prod_{i < j} (Z_i - Z_j)^{4m-4} \prod_{i, \gamma} (Z_i - z_\gamma)^{2m-1} \prod_{\gamma < \delta} (z_\gamma - z_\delta)^m \prod_{\gamma} e^{-|z_\gamma|^2/4l_0^2} \prod_i e^{-|Z_i|^2/2l_0^2}. \quad (2.31)$$

We note that the simplified wave function $\alpha \tilde{\phi}$ is just the schematic form stated without derivation in Ref. 8, as the starting point of the inductive derivation of fractional quasiparticle statistics. (Specifically, $\alpha \tilde{\phi}$ is equivalent to the wave function obtained by combining Eqs. (1) and (11) of Ref. 8, with the definitions $Q_0\{Z_k\} = \prod_{k < l} (Z_k - Z_l)^{-1}$, and $m_1 \equiv m = 2p_1 - 1$. The roles of upper- and lower-case position variables here are interchanged relative to Ref. 8.)

As noted in Ref. 8, if we take the trace of $|\tilde{\phi}|^2$ over the unpaired electron coordinates z_γ , the result has the form $|\tilde{\psi}[Z_i]|^2 \phi[Z_i]$, where

$$\begin{aligned} \tilde{\psi}[Z_i] = P(Z_i) \left[\prod_{i < j} |Z_i - Z_j|^{-1/m} \right] \\ \times \left[\prod_i e^{-|Z_i|^2/4ml_0^2} \right], \end{aligned}$$

while $\phi[Z_i]$ is the partition function of a classical one-component plasma with sources at positions Z_i . This partition function is independent of Z_i for large values of the separations, due to the screening property of the plasma. Thus, $|\tilde{\psi}[Z_i]|^2$ is, at least approximately, the probability of finding quasiparticles simultaneously at positions Z_i , and $\tilde{\psi}[Z_i]$ may be interpreted as a pseudo-wave function for the quasiparticles.

F. Wave function for the state $\nu=\frac{2}{3}$

If we are interested in stable states of particularly low energy, we should look for a state where the quasiparticles Z_i are uniformly spread out over the area occupied by the electrons, and kept away from each other as well as possible. By analogy with Laughlin's wave functions ψ_m , we would guess that a particularly good choice for the sym-

metric polynomial P is the product form

$$P(Z_i) = \prod_{i < j} (Z_i - Z_j)^{2p}, \quad (2.32)$$

where p is an integer ≥ 1 . Now $|\tilde{\psi}|^2$ is the distribution function of a classical statistical-mechanics problem with two kinds of particles, interacting with each other and with a uniform background charge density via logarithmic potentials of various strengths. The equivalent of the plasma neutrality requirement applied to each of the species results in the following equations, applicable in the region where both species are present:

$$(n - 2n_1)m + n_1(2m - 1) = \frac{1}{2\pi l_0^2}, \quad (2.33)$$

$$(n - 2n_1)(2m - 1) + n_1(2p + 4m - 4) = \frac{1}{\pi l_0^2}, \quad (2.34)$$

where n_1 is the density of pairs and $(n - 2n_1)$ the density of unpaired electrons. The solution of these equations

gives

$$\nu = 2\pi l_0^2 n = 2p / (2pm - 1), \quad (2.35)$$

$$2\pi l_0^2 (n - 2n_1) = 2(p - 1) / (2pm - 1). \quad (2.36)$$

These are the stable states at the second level of the quantized Hall hierarchy, obtained by adding quasiparticles to the fundamental states $\nu = 1/m$. We note that the choice $p = 1$ is a limiting case which gives

$$\nu = 2 / (m + 2), \quad (2.37)$$

$$n - 2n_1 = 0. \quad (2.38)$$

The last equation implies that there are no unpaired electrons in this case.

In the present paper we shall analyze the potential energy of the wave function ψ for the state $\nu = \frac{2}{5}$, which we obtain from (2.28), (2.29), and (2.32), with $p = 1$ and $m = 3$. Explicitly, we may write the trial wave function for the $\nu = \frac{2}{5}$ state in the form $\psi = \alpha \tilde{\psi}$, with

$$\tilde{\psi} = \left[\prod_k e^{-|z_k|^2 / 4l_0^2} \right] \left[\prod_{k < l} (z_k - z_l)^2 \right] \left[\prod_i (z_{2i} - z_{2i-1})^{-1} \right] \left[\prod_{i < j} (Z_i - Z_j)^2 \right], \quad (2.39)$$

where k and l run from 1 to N , while i and j run from 1 to $N_1 = N/2$, and Z_i is the center of gravity of the pair, as before.

The wave functions given by (2.28), (2.29), and (2.32) are actually special cases of some more general trial wave functions discussed originally in Ref. 4. For example, Eq. (2.39) above is a special case of Eq. (22) of Ref. 4, which may be written in the present notation as

$$\tilde{\psi} = \left[\prod_k e^{-|z_k|^2 / 4l_0^2} \right] \left[\prod_{k < l} (z_k - z_l)^s \right] \left[\prod_i (z_{2i-1} - z_{2i})^{-t} \right] \left[\prod_{i < j} (Z_i - Z_j)^{2u} \right], \quad (2.40)$$

where s , t , and u are required to be integers with $s > 0$, $u \geq 0$, $s - t > 0$, and $s - t$ odd. Also, u or t or both are required to be > 0 . It may be shown that this wave function leads to a filling factor $\nu = 2 / (2s + u)$.

As another example of Eq. (2.40), consider the choice $s = u = 1$, $t = 0$, which gives a filling factor $\nu = \frac{2}{3}$. From one point of view, this wave function may be considered an attempt to build a $\nu = \frac{2}{3}$ state by adding triply charged quasiparticles ($q = 1$) to the $\nu = \frac{1}{3}$ state.

As we are much more inclined to build the $\frac{2}{3}$ state by adding ordinary holes to the completely full Landau level, we might not expect *a priori* that this construction would lead to a very good wave function for the $\frac{2}{3}$ state. Another serious problem is that the choice $t = 0$ removes one of the factors that led to binding of the pairs in the case of the $\nu = \frac{2}{3}$ state, or the other examples given by Eq. (2.29) above. As a result the antisymmetrization operator α should have a much more drastic effect on this wave function than in the case of the $\nu = \frac{2}{3}$ state.

Despite the above reservations, we have attempted to evaluate the expectation value of the potential energy in

this trial wave function for the $\frac{2}{3}$ state—partly to test our Monte Carlo methods and partly to test the intuitive picture discussed above, which has motivated our choice of trial functions.

As will be discussed in Sec. III, the effect of antisymmetrization is indeed larger in the case $\nu = \frac{2}{3}$ than in the case $\nu = \frac{2}{5}$, and the leading antisymmetrization corrections to the energy have opposite sign in the two cases. (The corrections to the binding energy are -3% and 1% , respectively.) Nevertheless, the antisymmetrization seems well converged in both cases, and the value of the energy appears to be *closer* to the exact result in the case $\nu = \frac{2}{3}$ than for $\nu = \frac{2}{5}$.

We have also carried out simulations of Eq. (2.40) with $s = 3$, $t = 0$, and $u = 1$, corresponding to a filling factor $\nu = \frac{2}{7}$. We obtain a reasonable value of the energy, in this case, and the effects of antisymmetrization are quite small. The values of the energy differences between possible trial states for the $\nu = \frac{2}{7}$ state are also very small, however, and are smaller than the uncertainties in our calculation, so that no conclusion can be drawn.

III. COMPUTATIONAL METHODS AND NUMERICAL RESULTS

In this section we discuss the methods employed to compute energies and other properties of trial wave functions for the fundamental fractional quantized Hall states and excited states. As discussed in Sec. II, all these wave functions lead to statistical-mechanical problems related to that of the two-dimensional one-component plasma. For our calculations we have used the standard Metropolis Monte Carlo (MC) method.²¹ All computations were carried out on a CSPI MAP-300 array processor, which performs up to 4×10^6 floating point multiplications per second and twice as many additions in parallel. In Appendix B we illustrate the methods used to do efficient Monte Carlo calculations on such a machine.

Throughout this section, unless otherwise noted, distances will be measured in units of the "ion-disk radius" R_0 , which is defined for a uniform state of density \bar{n} as

$$R_0 = (\pi\bar{n})^{-1/2}. \quad (3.1)$$

For the fundamental states ψ_m , (2.2), this is related to the magnetic length l_0 by

$$R_0 = \sqrt{2m} l_0. \quad (3.2)$$

We also use (3.2) for the state with one quasiparticle or one quasihole. The contents of this section closely parallels Sec. II, where the trial functions were introduced.

A. Energy of the quantum Hall state $\nu = \frac{1}{3}$

It is straightforward to perform a Monte Carlo computation of the Coulomb energy (2.10) of the one-component plasma (2.3) and (2.4). The only problem is how to extract the thermodynamic limit of E/N from results using systems with a finite number of particles, N . Rather than working with periodic boundary conditions (associated with complications due to the long-range logarithmic interaction) or placing the system on the surface of a sphere in order to eliminate the effects of boundaries, we directly use the system defined by Eqs. (2.3) and (2.4), i.e., a disk-shaped system.

In Fig. 1 we show the results for E/N plotted as a function of $N^{-1/2}$ for systems with $N = 20, 30, 42, 72$, and 144 particles. The size of the vertical bars indicates the standard deviation, computed from between 12 (for $N = 144$) up to 80 (for $N = 20$) independent Monte Carlo simulations, each of which consists of between 50 000 ($N = 144$) and 160 000 ($N = 42$) Monte Carlo steps per particle. The results for E/N are fitted accurately by the polynomial

$$E/N \approx (-0.4101 + 0.06006/\sqrt{N} - 0.0423/N)e^2/l_0.$$

Using fits by first-, second-, and third-order polynomials in $N^{-1/2}$ leads to values (in units of e^2/l_0) for the thermodynamic limit of -0.4092 , -0.4101 , and -0.4099 , respectively, consistent with results by Levesque *et al.*,¹³ or about 1.2% higher than Laughlin's approximate result (-0.4156) based on solutions of hypernetted-chain equations.

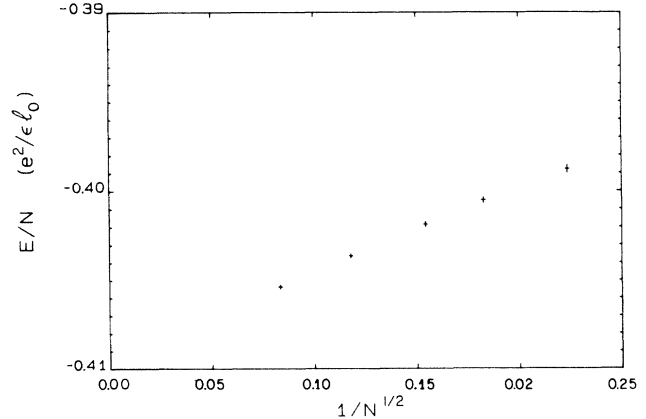


FIG. 1. Energy per electron E/N in the $\nu = \frac{1}{3}$ state. Results are based on Laughlin's trial wave function (2.2). Monte Carlo results for E/N are plotted versus $N^{-1/2}$ for systems with $N = 20, 30, 42, 72$, and 144 electrons. The length of the vertical bars indicates the standard deviation.

In order to compute directly the thermodynamic limit for the Coulomb energy per particle E/N , we can also make use of Eq. (2.7), in which E/N is expressed as an integral over the pair distribution function $g(r)$. For its computation we use a procedure which helps to efficiently eliminate the effects of the boundary: Let $\mathbf{r}_i^{(k)}$ be the position coordinates of particle i in the k th Monte Carlo step. We define our approximation $\hat{g}(r)$ for the pair distribution function $g(r)$ on a set of discrete separations $r_l = (l + \frac{1}{2})\Delta$ ($l = 0, 1, 2, \dots$) by

$$\hat{g}(r_l) = \frac{1}{2\pi\bar{n}\Delta} \frac{1}{N_{MC}} \sum_{k=1}^{N_{MC}} \frac{1}{N_1} \sum_{j=1}^N \sum_{i=1}^N \sum_{i \neq j}'' \frac{1}{|\mathbf{r}_i^{(k)} - \mathbf{r}_j^{(k)}|}, \quad (3.3)$$

where the summation \sum' includes all particles j which lie inside a circle around the origin with radius R_1 . N_1 denotes the average number of particles within this circle,

$$N_1 = \frac{1}{N_{MC}} \sum_{k=1}^{N_{MC}} \sum_{j=1}^N 1.$$

The summation \sum'' runs over all particles j whose separation $s = |\mathbf{r}_i^{(k)} - \mathbf{r}_j^{(k)}|$ from particle i lies in the interval

$$r_l - \Delta/2 \leq s < r_l + \Delta/2.$$

By N_{MC} we denote the number of Monte Carlo configurations. Note that in our units $\pi\bar{n} = 1$. The significance of definition (3.3) is twofold.

(i) By using only pairs, one member of which lies inside a circle of a radius R_1 around the origin, for a given r_l , $\hat{g}(r_l)$ will cease to be affected by the boundary, provided that the radius of the system $R > r_l + O(\xi)$, where ξ is the correlation length of the fluid.

(ii) The reason for binning with weight $|\mathbf{r}_i^{(k)} - \mathbf{r}_j^{(k)}|^{-1}$ (rather than with the more usual weight r_l^{-1}) is that, with

this definition, the computation of the Coulomb energy (2.7) can be carried out by direct summation of $[\hat{g}(r_i) - 1]$ without introducing discretization Δ -dependent integration errors.

In Fig. 2 we show plots of the pair distribution function for the state $\nu = \frac{1}{3}$ for systems with sizes $N = 30, 72,$ and 144 . Results are obtained from $5.6 \times 10^6, 2.4 \times 10^6,$ and 0.5×10^6 Monte Carlo steps per particle, respectively. For the discretization interval, a value $\Delta = \frac{1}{20}$ and a radius of the small circle $R_1 = R_0$ is used. As can be seen, there is, within statistical errors, no size dependence of $\hat{g}(r)$ in the 30-particle computations for $r < 2$, and for the 72-particle system for $r < 5$. This can be easily understood: The short-distance behavior of $g(r)$ shows that the correlation length ξ is of the order of about 3. We may expect that the effects of the boundary decay within about this same distance. For our choice $R_1 = R_0$ we expect that $\hat{g}(r)$ should only feel the effects of the boundaries for $r > R_N - (\xi + R_0)$. By R_N we denote the radius of a system with N particles, which, in units of the ion-disk radius R_0 , is given by $N^{1/2}$.

In Table I we list the values of the Coulomb energy per particle E/N [Eq. (2.7)] as a function of the upper limit of integration R , together with the values of the integral $C(R)$,

$$C(R) = 2 \int_0^R [\hat{g}(r) - 1] r dr, \quad (3.4)$$

which, owing to charge neutrality, must tend to -1 in the thermodynamic limit. We note that, provided that we use an upper cutoff R such that $C(R) = -1$, the size dependence of the results for the Coulomb energy E/N is very small, with values (in units of $e^2/\epsilon l_0$) of -0.4096 for $N = 42$ and 72 , and -0.4097 for the system with 144 particles. From these results we estimate the value in the thermodynamic limit to be

$$E/N \approx (-0.410 \pm 0.001) e^2/\epsilon l_0, \quad (3.5)$$

in close agreement with the Monte Carlo result by Levesque *et al.*,¹³ but slightly larger than Laughlin's result³ $(E/N)(\nu = \frac{1}{3}) \approx -0.4156 e^2/\epsilon l_0$, based on computations using hypernetted-chain equations.

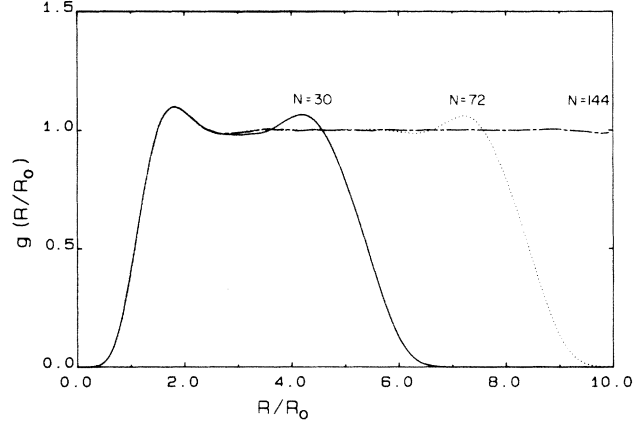


FIG. 2. Monte Carlo results for the radial distribution function $g(r)$ [Eq. (3.3)] for the system in the Laughlin $\nu = \frac{1}{3}$ state [Eq. (2.2)]. Results are based on calculations with $N = 30, 72,$ and 144 electrons.

B. Energy of the quasihole excitation in the $\nu = \frac{1}{3}$ state

Straightforward Monte Carlo simulation of the statistical-mechanical problem defined by Hamiltonian (2.14) for a quasihole at the origin ($\eta = 0$) in the $\nu = \frac{1}{3}$ state leads to results for the electron density $\langle n(r) \rangle$ plotted in Fig. 3.²² The density is calculated according to (3.3), but replacing $r_j^{(k)}$ by zero. We have used systems with $N = 30, 42,$ and 72 particles. The deficiency of $\frac{1}{3}$ electron at the origin is conspicuous. Indeed, the particle excess $X(R)$ defined by

$$X(R) = 2\pi \int [n(r) - \bar{n}] r dr \quad (3.6)$$

has values of $-0.340, -0.326,$ and -0.327 at $R = 2.5$ for the 30-, 42-, and 72-particle systems, respectively.

Let us now turn to the computation of the excitation energy. Consistent with the definition of proper energy $\bar{\epsilon}_-$ of a quasihole, described in Sec. IID, we must calculate the difference between the Coulomb energies $E_N^-(A)$ and $E_N(A)$ of systems with the same number of particles N , with and without a quasihole, occupying the same physical area A , but with slightly different values of the

TABLE I. Energy per particle E/N of the $\nu = \frac{1}{3}$ state. Shown are Monte Carlo results for E/N , calculated by integrating the radial distribution function $g(r)$ (cf. Fig. 2) up to an upper cutoff R_{\max} ; also listed are results for the integral $C(R_{\max})$ [Eq. (3.4)], which in the bulk limit tends to -1 . Choosing $R_{\max} > 4$ such that $C(R_{\max}) = -1$, yields the results in the second line from the bottom. (Config. denotes configurations.)

R_{\max}	$N = 42$		$N = 72$		$N = 144$	
	$C(R_{\max})$	E/N	$C(R_{\max})$	E/N	$C(R_{\max})$	E/N
3.2	-1.0062	-0.4101	-1.0059	-0.4099	-1.0072	-0.4101
4	-0.9993	-0.4096	-1.0015	-0.4097	-0.9975	-0.4096
5	-0.9711	-0.4088	-0.9996	-0.4096	-0.9985	-0.4096
6	-1.1328	-0.4132	-0.9983	-0.4095	-0.9993	-0.4097
	-1	-0.4096	-1	-0.4096	-1	-0.4097
Config.	1.2×10^6		0.96×10^6		0.48×10^6	

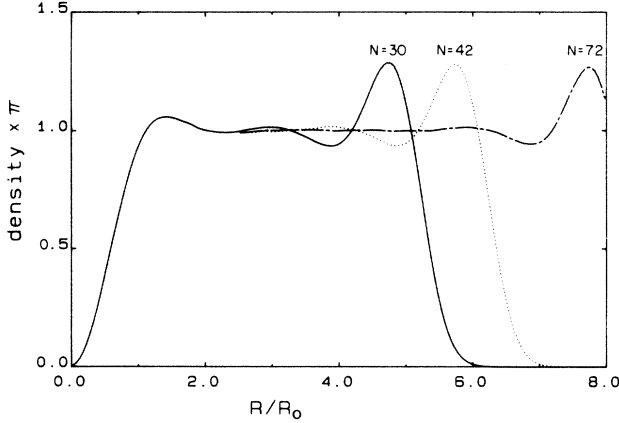


FIG. 3. Electron density $\langle n(r) \rangle$ in the Laughlin quasihole state (2.12) at $\nu = \frac{1}{3}$, for systems with $N = 30, 42,$ and 72 electrons. Note that apart from the width of the flat regime, results are essential independent of N .

magnetic field. In the present section, however, we have chosen to measure all distances in terms of the ion-disk radius $R_0 = (2m)^{1/2}l_0$, so we will have to correct for the difference in the magnetic length l_0 .

In each case, we first calculate the Coulomb energy of the finite system, at Monte Carlo step k , according to the prescription

$$E_N^{(k)} = \frac{e^2}{\epsilon} \sum_{\substack{i,j=1 \\ i < j}}^N \frac{1}{|\mathbf{r}_i^{(k)} - \mathbf{r}_j^{(k)}|} + \sum_{i=1}^N U_B(\mathbf{r}_i^{(k)}) + E_{BG}(N), \quad (3.7)$$

where $U_B(\mathbf{r})$ is the energy of an electron at position \mathbf{r} , interacting with the positive background,

$$U_B(\mathbf{r}) = -\frac{e^2}{\epsilon} \int_{|\mathbf{r}'| \leq R_B} \frac{\bar{n}}{|\mathbf{r} - \mathbf{r}'|} d^2r', \quad (3.8)$$

and $E_{BG}(N)$ is the energy of the background,

$$E_{BG}(N) = \frac{e^2 \bar{n}^2}{2\epsilon} \int_{|\mathbf{r}| \leq R_B} \int_{|\mathbf{r}'| \leq R_B} \frac{d^2r d^2r'}{|\mathbf{r}' - \mathbf{r}|}. \quad (3.9)$$

In these equations, R_B is the radius of the neutralizing background disk, and $\bar{n} \equiv N/(\pi R_B^2)$. For the system in the fundamental state $\nu = 1/m$, we choose

$$R_B = N^{1/2} \equiv (A/\pi)^{1/2}, \quad (3.9a)$$

while for the system with the quasihole we choose

$$R_B = (N + 1/m)^{1/2} \equiv (A'/\pi)^{1/2}. \quad (3.9b)$$

We identify the energy $E_N(A)$ with the average $\langle E_N^{(k)} \rangle$ of the Monte Carlo energies for the fundamental state, while for the quasihole we write

$$E_N^-(A) = (A'/A)^{1/2} E_N^-(A'),$$

where $E_N^-(A')$ is the average of the Monte Carlo energies, $\langle E_N^{(k)} \rangle$, for the system with the quasihole.

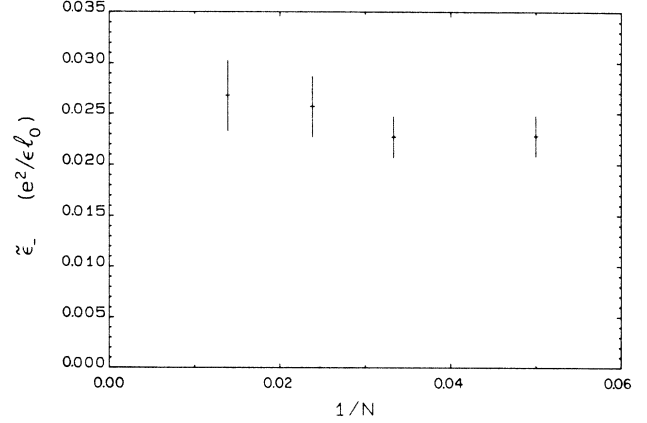


FIG. 4. Proper energy $\bar{\epsilon}_-$ of quasihole excitation in the $\nu = \frac{1}{3}$ state. Monte Carlo results for $\bar{\epsilon}_-$ are plotted versus N^{-1} for systems with $N = 20, 30, 42,$ and 72 electrons.

We have carried out computations at $m = 3$, using systems with $N = 20, 30, 42,$ and 72 particles. The differences $E_N^-(A) - E_N(A)$ give our estimates for the quasihole energy $\bar{\epsilon}_-(\frac{1}{3})$, which we finally express in units of $e^2/\epsilon l_0$, where l_0 is the magnetic length of the fundamental state.

In Fig. 4 we plot the results for $\bar{\epsilon}_-$ based on MC computations using systems with $N = 20, 30, 42,$ and 72 particles. The standard deviation, computed from the results of, respectively, 80, 56, 40, and 24 independent MC simulations, with between 40000 and 100000 Monte Carlo steps per particle, is indicated by the length of the vertical bars. Note that for the $N = 72$ system an accuracy in $\bar{\epsilon}_-$ of 0.001 would require the computation of the electron-electron interaction energy (3.7) to a precision of 1 in 2^{18} , i.e., only about 1.5 orders of magnitude below the limits of the arithmetic precision of the MAP array processor, whose mantissa has 24 bits. Owing to the large statistical errors we are unable to perform a reliable extrapolation to the thermodynamic limit. However, results of $\bar{\epsilon}_- \approx 0.025 - 0.027e^2/\epsilon l_0$ for systems with 42 and 72 particles are consistent with Laughlin's result $\bar{\epsilon}_- \approx 0.026e^2/\epsilon l_0$, based on solution of modified hypernetted-chain equations.³

C. Energy of a quasiparticle in the $\nu = \frac{1}{3}$ state

In this subsection we present the results of computations based on the two types of trial wave functions (2.17) and (2.18) for a quasiparticle in the $\nu = \frac{1}{3}$ state.

1. Laughlin's trial wave function (2.17)

As first discussed by Laughlin,⁷ the absolute square of wave function (2.17) can be written in the form of a distribution function of a generalized statistical-mechanical problem. Making use of the identity

$$\left| 2 \frac{dP}{dZ} \right|^2 = \nabla^2 |P|^2,$$

which holds for any polynomial $P(z)$, the two-particle density $\langle n(\mathbf{r}_1)n(\mathbf{r}_2) \rangle$ takes the form

$$\langle n(\mathbf{r}_1)n(\mathbf{r}_2) \rangle = \frac{\int |\psi|^2 d^2r_3 d^2r_4 \cdots d^2r_N}{\int |\psi|^2 d^2r_1 d^2r_2 \cdots d^2r_N}, \quad (3.10)$$

with

$$|\psi|^2 = \prod_{j=1}^N \left[e^{-mr_j^2} \frac{1}{4m^2} \nabla_j^2 \right] \exp \left[2m \sum_{i < k} \ln |\mathbf{r}_i - \mathbf{r}_k| \right]. \quad (3.11)$$

Integrating by parts, the Laplacians in the integrals (3.10) can be eliminated,

$$\langle n(\mathbf{r}_1)n(\mathbf{r}_2) \rangle = \frac{1}{Z} e^{-m(r_1^2+r_2^2)} \frac{\nabla_1^2 \nabla_2^2}{16m^4} \int \prod_{j=3}^N \left[d^2r_j \left[r_j^2 - \frac{1}{m} \right] e^{-mr_j^2} \right] \exp \left[2m \sum_{i < k} \ln |\mathbf{r}_i - \mathbf{r}_k| \right], \quad (3.12)$$

where $Z = \text{Tr} e^{-K}$ is the partition function of a generalized (complex) Hamiltonian K , given by

$$e^{-K} = e^{-H_m} \prod_{j=1}^N \left[r_j^2 - \frac{1}{m} \right], \quad (3.13)$$

and H_m is the one-component plasma Hamiltonian (2.4). Equation (3.12) for the two-particle density can be brought into a better readable form. Using the notation $X_i = e^{mr_i^2}$ and defining the expectation value $\langle\langle O \rangle\rangle_K$ of operator O in the state (3.13) by

$$\langle\langle O \rangle\rangle_K = Z^{-1} \text{Tr}(Oe^{-K}), \quad (3.14)$$

Eq. (3.12) may be rewritten as

$$\langle n(\mathbf{r}_1)n(\mathbf{r}_2) \rangle = \frac{X_1^{-1} X_2^{-1}}{16m^4} \nabla_1^2 \nabla_2^2 \left[\frac{X_1}{r_1^2 - 1/m} \frac{X_2}{r_2^2 - 1/m} \langle\langle n(\mathbf{r}_1)n(\mathbf{r}_2) \rangle\rangle_K \right], \quad (3.15)$$

where $\langle\langle n(\mathbf{r}_1)n(\mathbf{r}_2) \rangle\rangle_K$ is the two-particle density of a system, defined by the generalized Hamiltonian K . A similar derivation leads to an expression for the density $\langle n(\mathbf{r}_1) \rangle$,

$$\langle n(\mathbf{r}_1) \rangle = X_1^{-1} \frac{\nabla_1^2}{4m^2} \left[\frac{X_1}{r_1^2 - 1/m} \langle\langle n(\mathbf{r}_1) \rangle\rangle_K \right], \quad (3.16)$$

which after elimination of $X_1 = \exp(mr_1^2)$ can be put into the form

$$\langle n(\mathbf{r}_1) \rangle = \left[\frac{1}{4m^2} \nabla_1^2 + \frac{1}{m} \mathbf{r}_1 \cdot \nabla_1 + r_1^2 + \frac{1}{m} \right] f(\mathbf{r}_1), \quad (3.17)$$

with

$$f(\mathbf{r}_1) = \frac{\langle\langle n(\mathbf{r}_1) \rangle\rangle_K}{r_1^2 - 1/m}. \quad (3.18)$$

In his computation,⁷ Laughlin made use of expression (3.16) for the density $\langle n(\mathbf{r}) \rangle$. Using an approximate method he computed $\langle n(\mathbf{r}) \rangle$ and determined a pseudopotential for use in a type of hypernetted-chain equation, consistent with the already known $\langle n(\mathbf{r}) \rangle$. By this set of approximations he gets a value $\tilde{\epsilon}_+(\frac{1}{3}) \approx 0.03e^2/\epsilon l_0$ for the proper energy of a quasiparticle. Chakraborty⁹ has carried out an analysis quite similar to Laughlin's, and reports a slightly lower energy, $\tilde{\epsilon}_+(\frac{1}{3}) \approx 0.025$.

In our present work we also make use of expressions (3.15) and (3.17) for the two- and one-particle densities. However, we do not make any approximations, calculating the expectation values $\langle\langle O \rangle\rangle_K$ by Monte Carlo importance sampling.

The difficulty associated with the fact that the probability density e^{-K} is not positive is handled by treating its sign separately. Using the decomposition

$$e^{-K} = e^{-\tilde{K}} S, \quad (3.19)$$

where

$$e^{-\tilde{K}} = e^{-H_m} \prod_{j=1}^N \left[r_j^2 - \frac{1}{m} \right] \quad (3.20)$$

and

$$S = \text{sgn} \left[\prod_{j=1}^N \left[r_j^2 - \frac{1}{m} \right] \right], \quad (3.21)$$

the required expectation values $\langle\langle O \rangle\rangle_K$ take the form

$$\langle\langle O \rangle\rangle_K = \frac{\text{tr}(OS e^{-\tilde{K}})}{\text{tr}(S e^{-\tilde{K}})} = \frac{\langle\langle OS \rangle\rangle_{\tilde{K}}}{\langle\langle S \rangle\rangle_{\tilde{K}}}, \quad (3.22)$$

and can be readily computed by standard Monte Carlo

procedure in which the generation of configurations is controlled by the less unusual Hamiltonian \tilde{K} ,

$$\tilde{K} = H_m - \sum_{j=1}^N \ln \left| r_j^2 - \frac{1}{m} \right|. \quad (3.23)$$

Although Hamiltonian K becomes singular whenever an electron approaches the edge, it can be handled in a straightforward manner by Monte Carlo importance sampling. Standard molecular-dynamics simulation, on the other hand, would preclude particles from entering or leaving the disk, and special tricks would be required designed to allow the system to equilibrate.

The computation of the density $\langle n(\mathbf{r}) \rangle$, (3.17), proceeds as follows: Binning the values of

$$S^{(k)} / \left[\left| \left(\mathbf{r}_i^{(k)} \right)^2 - \frac{1}{m} \right| \cdot \left| \mathbf{r}_i^{(k)} \right| \right],$$

where $S^{(k)}$ stands for the value of the sign operator S in Monte Carlo step k , we form [cf. Eq. (3.3)]

$$\tilde{f}^{(k)}(r_l) = \frac{1}{2\pi\bar{n}\Delta} \sum_{i=1}^N \frac{S^{(k)}}{\left| \mathbf{r}_i^{(k)} \right| \left[\left(\mathbf{r}_i^{(k)} \right)^2 - 1/m \right]}. \quad (3.24)$$

The summation is over all particles i whose distance $s = \left| \mathbf{r}_i^{(k)} \right|$ from the origin lies in the interval $r_l - \Delta/2 \leq s < r_l + \Delta/2$. Performing an average over N_{MC} Monte Carlo steps, we get a Monte Carlo approximation $\tilde{f}(r)$ to $f(r)$, (3.18),

$$\tilde{f}(r_l) = \frac{\sum_{k=1}^{N_{MC}} \tilde{f}^{(k)}(r_l)}{\sum_{k=1}^{N_{MC}} S^{(k)}}, \quad (3.25)$$

defined on points $r_l = (l + \frac{1}{2})\Delta$.

In Fig. 5 we show a plot of $\tilde{n}(\mathbf{r}) = (\mathbf{r}^2 - 1/m)\tilde{f}(r)$ [Eq. (3.18)] for a system with $N=30$ particles. Open circles are the Monte Carlo results, while the solid line represents an interpolation using a Padé approximation to $\tilde{f}(r)$,

$$\tilde{f}(r) \cong (a_0 + a_1 r^2 + a_2 r^4) / (1 + b_1 r^2), \quad (3.26)$$

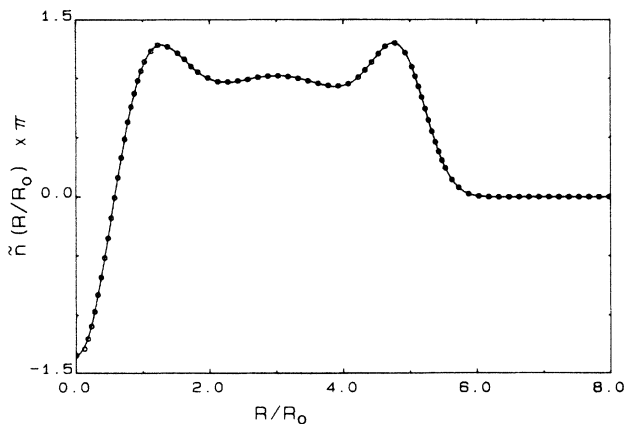


FIG. 5. Laughlin quasiparticle state at $\nu = \frac{1}{3}$: Unphysical density $\tilde{n}(\mathbf{r}) = \langle n(\mathbf{r}) \rangle_K$ resulting from generalized Hamiltonian K [Eq. (3.13)]; open circles are Monte Carlo results, and the solid line corresponds to a fit based on Eq. (3.26). A system with $N=30$ electrons is used.

and a third-order spline polynomial for $r > 1.2$. Padé coefficients are $a_0 = 4.05112$, $a_1 = -2.08448$, $a_2 = 0.38863$, and $b_1 = 0.42435$. Using this fit to $\tilde{f}(r)$ in Eq. (3.17) results in a density $\langle n(r) \rangle$ plotted in Fig. 6.

Shown are results from computations using 30, 42, and 72 particles. We note that the excess charge is located inside a circle of radius $R \approx 2$ with a pronounced dip at the origin. We have attempted to verify if the value slightly below 1 at the origin may not be the result of an inadequate choice of the interpolation function (3.26). Varying the degree of the numerator and/or denominator polynomials and the range of fitting ($r < 0.7$ up to $r < 1.4$) does not change the behavior at the origin of $\langle n(r) \rangle$ in a significant way. A dip in the charge density at the quasiparticle state has previously been noted by Haldane and Rezayi,¹¹ but their charge density does not drop below 1, as ours does.

For the 72-particle systems, the particle excess $X(R)$ [Eq. (3.6)] has values of 0.207, 0.408, and 0.330 at $R = 1, 2$, and 3, respectively, and for $3 < R < 6$ it oscillates around the value $\frac{1}{3}$, as required.

For the computation of the Coulomb energy $E_N^+(A)$ of a system with a quasiparticle, we insert the expressions for the two- and one-particle densities [Eqs. (3.15) and (3.17)] into the definition of the Coulomb energy (2.10) and (2.11). Integrating by parts, the Laplacians can be made to act on the Coulomb potential. This leads to expressions

$$E_{pp}^{(k)} = \sum_{i < j} \frac{1}{\left[\left(\mathbf{r}_i^{(k)} \right)^2 - 1/m \right] \left[\left(\mathbf{r}_j^{(k)} \right)^2 - 1/m \right]} \times D_i D_j \frac{1}{\left| \mathbf{r}_i^{(k)} - \mathbf{r}_j^{(k)} \right|} \quad (3.27)$$

for the electron-electron interaction energy in Monte Carlo step k , and

$$E_{pB}^{(k)} = \sum_i \frac{1}{\left(\mathbf{r}_i^{(k)} \right)^2 - 1/m} D_i U_B'(\mathbf{r}_i^{(k)}) + E_{BG}' \quad (3.28)$$

for the electron-background interaction, including the

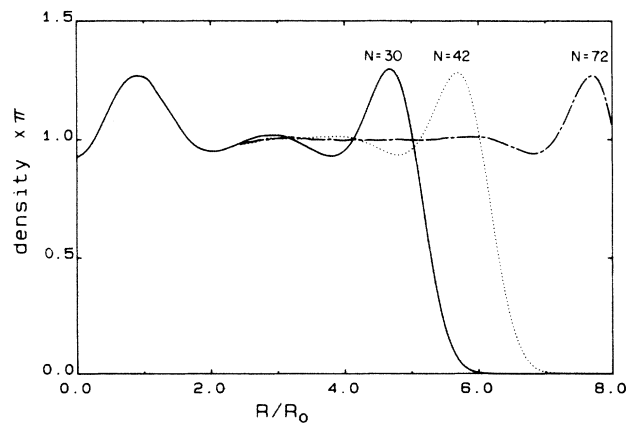


FIG. 6. Electron density $\langle n(\mathbf{r}) \rangle$ in the Laughlin quasiparticle state $\nu = \frac{1}{3}$. Results are obtained from Monte Carlo values for unphysical density $\tilde{n}(\mathbf{r})$ (cf. Fig. 5), using Eqs. (3.17) and (3.18).

background energy E'_{BG} . We have used the notation

$$D_i = \frac{1}{4m^2} \nabla_i^2 - \frac{1}{m} \mathbf{r}_i \cdot \nabla_i + r_i^2 - \frac{1}{m}. \quad (3.29)$$

In (3.28) the primes (U'_B and E'_{BG}) indicate the use of a background with radius $R_B \equiv (A'/\pi)^{1/2} = (N-1/m)^{1/2}$.

Since, however, $D_i U'_B(\mathbf{r}_i)$ has a singular behavior at the edge of the disk (if a sharp cutoff is used for the charge density of the positive background), we have split $U'_B(\mathbf{r}_i)$ into a polynomial part $\tilde{U}'_B(\mathbf{r}_i)$.

$$\tilde{U}'_B(r) = -2\pi\bar{n}e^2 R_B \sum_{n=0}^5 a_n \left(\frac{r}{R_B} \right)^{2n},$$

whose contribution is evaluated using Eq. (3.28) and a remainder $U'_B - \tilde{U}'_B$, which we evaluate by integration over the density [Eqs. (2.10), (2.11), and (3.17)]. The coefficients a_n are $a_0=1$, $a_1=-0.25917$, $a_2=0.06052$, $a_3=-0.44160$, $a_4=-0.65545$, and $a_5=-0.37709$.

The required Coulomb energy $E_N^+(A)$ is then obtained by performing an average over N_{MC} Monte Carlo steps, and rescaling according to the discussion in Sec. III B:

$$E_N^+(A) = \left(\frac{A'}{A} \right)^{1/2} \frac{\sum_{k=1}^{N_{MC}} S^{(k)} (E_{pp}^{(k)} + E_{pB}^{(k)})}{\sum_{k=1}^{N_{MC}} S^{(k)}}, \quad (3.30)$$

where $A'/A = (Nm-1)/Nm$.

In Fig. 7 we plot the results for $\tilde{\epsilon}_+$ from computations with systems with 20, 30, 42, and 72 particles. Standard deviation is obtained from 80, 56, 40, and 24 independent MC simulations, respectively. Results are derived from a total of 6.4×10^6 , 5.6×10^6 , 7.2×10^6 , and 3×10^6 Monte Carlo steps per particle, respectively. We cannot reliably extrapolate these results for $\tilde{\epsilon}_+$ to the thermodynamic limit, but a plausible estimate is

$$\tilde{\epsilon}_+ \approx (0.073 \pm 0.008) e^2 / \epsilon l_0, \quad (3.31)$$

and as a value for the gap $E_g = \tilde{\epsilon}_+ + \tilde{\epsilon}_-$ we list its value

obtained for the $N=72$ electron system,

$$E_g = \tilde{\epsilon}_+ + \tilde{\epsilon}_- \approx (0.0966 \pm 0.0050) e^2 / \epsilon l_0. \quad (3.32)$$

In any case, our results do not agree with Laughlin's results⁷ $\tilde{\epsilon}^+(\frac{1}{3}) \approx 0.03 e^2 / \epsilon l_0$, and give reason to doubt the validity of the approximations made in that calculation.

The operator S [Eq. (3.21)] has an expectation value

$$\langle\langle S \rangle\rangle_{\bar{K}} \approx 0.708 \pm 0.002, \quad (3.33)$$

which implies that in somewhat less than 15% of the configurations, one electron is located inside the disk $r^2 \leq \frac{1}{3}$. The large value of $\langle\langle S \rangle\rangle_{\bar{K}}$ ensures that there is no loss of accuracy due to the division of (3.22).

2. One pair trial wave function (2.18)

Monte Carlo simulation of a system described by the classical Hamiltonian \tilde{H} defined in Eq. (2.20) allows one to study directly the properties of the nonsymmetrized wave function $\tilde{\psi}_0^{(+)}$ of Eq. (2.18b). The mean density $\langle \tilde{\psi}_0^{(+)} | n(\mathbf{r}) | \tilde{\psi}_0^{(+)} \rangle$ is plotted in Fig. 8 for systems with $N=20, 30$, and 42 particles. The excess charge accumulated around the origin is conspicuous; however, the detailed shape of $\langle n(\mathbf{r}) \rangle$ is very different from the one obtained using Laughlin's trial wave function for a quasiparticle (cf. Fig. 6). Since $\tilde{\psi}_0^{(+)}$ is not fully antisymmetric, however, it is important to study the effects of the antisymmetrizer α in (2.18a). Let us write

$$\alpha = \sum_P (-1)^{|P|} P, \quad (3.34)$$

where P stands for a permutation of N particles and $(-1)^{|P|}$ is its sign. Using this expansion of the antisymmetrizer α , expectation values $\langle O \rangle$ of an operator O in the fully antisymmetrized state $\psi_0^{(+)} = \alpha \tilde{\psi}_0^{(+)}$ can be calculated as follows. We note that

$$\langle O \rangle = \langle \psi_0^{(+)} | O | \psi_0^{(+)} \rangle / \langle \psi_0^{(+)} | \psi_0^{(+)} \rangle \quad (3.35)$$

can be expressed in terms of integrals of the form

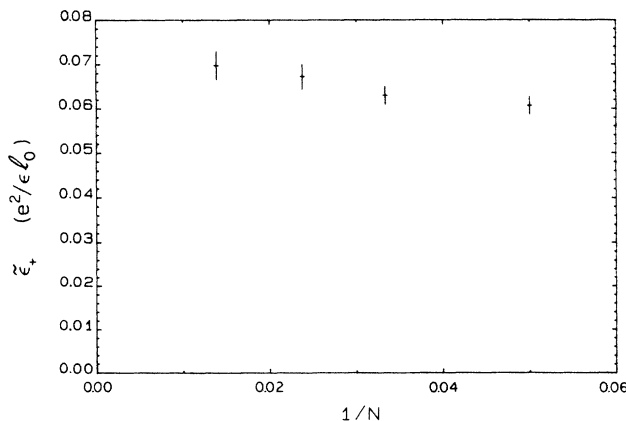


FIG. 7. Quasiparticle energy $\tilde{\epsilon}_+$ in the $\nu = \frac{1}{3}$ state. For the state containing the quasiparticle excitation, the Laughlin derivative wave function (2.17) is used.

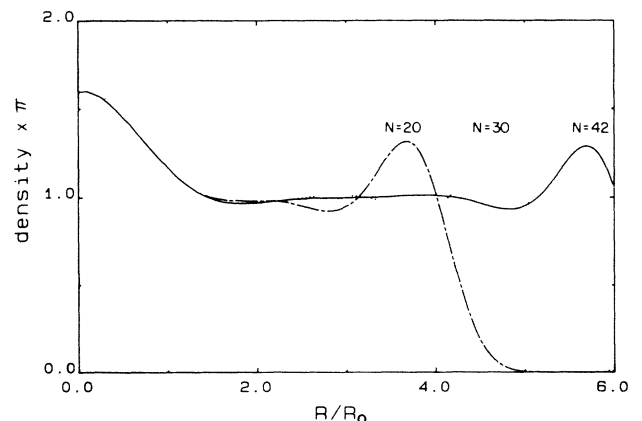


FIG. 8. Density $\langle n(\mathbf{r}) \rangle$ in the state with quasiparticle excitation at $\nu = \frac{1}{3}$. The Monte Carlo result is based on the nonsymmetrized pair wave function $\tilde{\psi}_0^{(+)}$ [Eq. (2.18b)].

$$\langle \tilde{\psi}_0^{(+)} | P'OP | \tilde{\psi}_0^{(+)} \rangle .$$

For a symmetric operator O , satisfying $PO=OP$ for any permutation P , the term $(-1)^{|P|} \langle P\tilde{\psi}_0^{(+)} | O | \psi_0^{(+)} \rangle$ in the expansion of $\langle a\tilde{\psi}_0^{(+)} | O | \psi_0^{(+)} \rangle$ contributes a value $(-1)^{|P|} \langle \tilde{\psi}_0^{(+)} | O | P\psi_0^{(+)} \rangle$, which, owing to the antisymmetry of ψ_0^{+} , is given by $\langle \tilde{\psi}_0^{(+)} | O | \psi_0^{(+)} \rangle$, independent of permutation P . Applying this consideration to both numerator and denominator in (3.33), the expectation value $\langle O \rangle$ of a symmetric operator O can be written as

$$\langle O \rangle = \frac{\langle \tilde{\psi}_0^{(+)} | Oa | \tilde{\psi}_0^{(+)} \rangle}{\langle \tilde{\psi}_0^{(+)} | a | \tilde{\psi}_0^{(+)} \rangle} . \quad (3.36)$$

Its computation requires evaluation of integrals of the form $\langle \tilde{\psi}_0^{(+)} | OP | \tilde{\psi}_0^{(+)} \rangle$. Defining the ratio $R_P[z_i]$,

$$R_P[z_i] = P\tilde{\psi}_0^{(+)}[z_i] / \tilde{\psi}_0^{(+)}[z_i] , \quad (3.37)$$

we may write

$$\frac{\langle \tilde{\psi}_0^{(+)} | OP | \tilde{\psi}_0^{(+)} \rangle}{\langle \tilde{\psi}_0^{(+)} | \tilde{\psi}_0^{(+)} \rangle} = \frac{\text{Tr}(OR_P e^{-\beta\tilde{H}})}{\text{Tr}e^{-\beta\tilde{H}}} , \quad (3.38)$$

in a form suited for computation by means of Monte Carlo importance sampling according to the distribution $|\tilde{\psi}_0^{(+)}|^2 = e^{-\beta\tilde{H}}$.

Let us now discuss the antisymmetrizer a . Due to the fact that $\tilde{\psi}_0^{+}$ is already fully antisymmetric with respect to particles 3, . . . , N , and also antisymmetric under interchange of the positions of particles 1 and 2, the antisymmetrizer a takes the form

$$a = 1 + a^{(1)} + a^{(2)} , \quad (3.39)$$

with

$$a^{(1)} = - \sum_{k \geq 3}^N (P_{1k} + P_{2k}) \quad (3.40)$$

and

$$a^{(2)} = \sum_{l > k \geq 3} P_{lk} P_{2l} . \quad (3.41)$$

Operator P_{ik} interchanges the positions of particles i and k . Using expression (3.39) for the antisymmetrizer, the expectation value $\langle O \rangle$, (3.36), can be expanded as

$$\langle O \rangle = \langle\langle O \rangle\rangle + \Delta^{(1)} + \Delta^{(2)} , \quad (3.42)$$

where $\Delta^{(1)}$ and $\Delta^{(2)}$ are corrections due to two- and four-

particle exchanges $a^{(1)}$ and $a^{(2)}$, respectively,

$$\Delta^{(i)} = \frac{\langle\langle Oa^{(i)} \rangle\rangle - \langle\langle O \rangle\rangle \langle\langle a^{(i)} \rangle\rangle}{\langle\langle 1 + a^{(1)} + a^{(2)} \rangle\rangle} . \quad (3.43)$$

Here, we use the definition

$$\langle\langle Q \rangle\rangle = \frac{\langle \tilde{\psi}_0^{(+)} | Q | \tilde{\psi}_0^{(+)} \rangle}{\langle \tilde{\psi}_0^{(+)} | \tilde{\psi}_0^{(+)} \rangle} \quad (3.44)$$

for arbitrary operator Q , e.g., sums of permutation operators P or OP .

In Table II we list results of computations of the quasiparticle energy $\tilde{\epsilon}_+$ in the $\nu = \frac{1}{3}$ state. Systems with $N=20, 30$, and 42 particles are used. The energy of an N -particle system occupying area $A = \pi R_N^2 = \pi N$ is denoted by $E_N(A)$ for the reference system without a quasiparticle and by $E_N^{+(0)} = E_N(A) + \tilde{\epsilon}_+^{(0)}$ for the system in the nonantisymmetrized state $\tilde{\psi}_0^{+}$.

As can be seen, corrections $\Delta^{(1)}$ and $\Delta^{(2)}$ [(3.42) and (3.43)] both reduce the energy, resulting in values of the proper energy $\tilde{\epsilon}_+$ of the quasiparticle in close agreement with those obtained using Laughlin's trial wave function (2.17) (cf. Fig. 7). Note that the correction $\Delta^{(2)}$ due to four-particle exchanges is about a factor of 5 smaller than the leading correction $\Delta^{(1)}$. Better statistics are required to determine the size dependence of these quantities. This will be difficult to achieve since the results for the 42-particle system required more than four weeks of computation time on the MAP-300.

Let us now return to the behavior of the density. In order to study antisymmetrization effects on its shape, we compute the expectation value $\langle O(\alpha) \rangle$ of operator $O(\alpha)$,

$$O(\alpha) = \frac{1}{\alpha^2} \sum_{i=1}^N e^{-r_i^2/\alpha^2} , \quad (3.45)$$

which measures the behavior of the density near the origin. Its expectation value $\langle O(\alpha) \rangle$ is related to the density $\langle n(r) \rangle$ by

$$\langle O(\alpha) \rangle = \frac{2\pi}{\alpha^2} \int e^{-(r/\alpha)^2} \langle n(r) \rangle r dr , \quad (3.46)$$

and is equal to unity in the system without a defect. In Table III we list results for $\langle O(\alpha) \rangle$, based both on Laughlin's trial wave function (2.17) and on the pair trial wave function (2.18) with and without antisymmetrization corrections $\Delta^{(1)}$ and $\Delta^{(2)}$ resulting from contributions $a^{(1)}$, (3.40), and $a^{(2)}$, (3.41), to the antisymmetrizer a , (3.39).

TABLE II. Proper energy $\tilde{\epsilon}_+$ of quasiparticle excitation at $\nu = \frac{1}{3}$. Results for $\tilde{\epsilon}_+^{(0)}$ and $\tilde{\epsilon}_+$ are based on pair wave functions $\tilde{\psi}_0^{(+)}$ and $\psi_0^{(+)} = a\tilde{\psi}_0^{+}$ [Eq. (2.18)], the latter being fully antisymmetrized. Corrections to the energy $\Delta^{(1)}$ and $\Delta^{(2)}$ [Eq. (3.43)] from two- and four-particle interchanges $a^{(1)}$ and $a^{(2)}$ [Eqs. (3.40) and (3.41)] are also listed, as well as contributions to the normalization of the wave function, $\langle\langle a^{(1)} \rangle\rangle$ and $\langle\langle a^{(2)} \rangle\rangle$. Results are from Monte Carlo calculations with systems of 30 electrons. Standard deviation of the last digit is indicated by numbers in parentheses. (Config. denotes configurations.)

N	Config.	$\tilde{\epsilon}_+^{(0)}$	$\langle\langle a^{(1)} \rangle\rangle$	$\langle\langle a^{(2)} \rangle\rangle$	$\Delta^{(1)}$	$\Delta^{(2)}$	$\tilde{\epsilon}_+$
20	1.8×10^6	0.103(4)	0.728(20)	0.064(27)	-0.038(4)	-0.008(4)	0.058(7)
30	1.9×10^6	0.103(2)	0.709(9)	0.092(27)	-0.036(3)	-0.006(3)	0.061(5)
42	1.5×10^6	0.107(3)	0.732(23)	0.092(30)	-0.033(3)	-0.008(4)	0.066(6)

TABLE III. Gaussian weighted integrals $O(\alpha)$ [Eq. (3.46)] of density $\langle n(\mathbf{r}) \rangle$ in the quasiparticle state at $\nu = \frac{1}{3}$. Monte Carlo results $\langle O(\alpha) \rangle_{\text{NA}}$ and $\langle O(\alpha) \rangle_P$ are based on the nonantisymmetrized pair wave function $\tilde{\psi}_0^{(+)}$ and fully antisymmetric $\psi_0^{(+)} = \alpha \tilde{\psi}_0^{(+)}$ [Eq. (2.18)], respectively. $\langle O(\alpha) \rangle_L$ refers to results for the Laughlin derivative wave function (2.17). Also listed are the antisymmetrization corrections $\Delta_\alpha^{(1)}$ and $\Delta_\alpha^{(2)}$ resulting from two- and four-particle interchanges $\alpha^{(1)}$ and $\alpha^{(2)}$ [Eqs. (3.40) and (3.41)]. Systems of $N = 30$ electrons are used.

α	$\langle O(\alpha) \rangle_{\text{NA}}$	Wave function		$\langle O(\alpha) \rangle_P$	Laughlin $\langle O(\alpha) \rangle_L$
		Pair type $\Delta_\alpha^{(1)}$	$\Delta_\alpha^{(2)}$		
0.601	1.422(3)	-0.183(6)	-0.072(14)	1.167(17)	1.126(8)
0.849	1.317(1)	-0.090(4)	-0.033(8)	1.194(10)	1.159(3)
1.201	1.204(1)	-0.030(2)	-0.010(3)	1.164(4)	1.140(1)

Results are obtained using a system with 42 particles. Note that both correction terms $\Delta_\alpha^{(1)}$ and $\Delta_\alpha^{(2)}$ reduce the expectation value of $O(\alpha)$, the contribution from four-particle interchanges, $\Delta_\alpha^{(2)}$, being only a factor of 2.5 smaller than the leading correction $\Delta_\alpha^{(1)}$. The slight increase of the values of $\langle O(\alpha) \rangle$ from 1.167 for $\alpha = 0.601$ to 1.194 at $\alpha = 0.849$ again implies a dip in the density at the origin for the system described by the fully antisymmetrized pair wave function $\psi_0^{(+)}$, Eq. (2.18).

Results for the Laughlin wave function are based on the same method used to compute the electron-background interaction (3.28). Using the notation

$$\tilde{O}(\alpha) = \frac{1}{\alpha^2} \sum_i \frac{1}{r_i^2 - 1/m} D_i \exp \left[-\frac{1}{\alpha^2} r_i^2 \right], \quad (3.47)$$

where the operator D_i is defined by Eq. (3.29), the expectation value $\langle O(\alpha) \rangle$ in the Laughlin quasiparticle state is given by

$$\langle O(\alpha) \rangle = \frac{\sum_{k=1}^{N_{\text{MC}}} S^{(k)} \tilde{O}^{(k)}(\alpha)}{\sum_{k=1}^{N_{\text{MC}}} S^{(k)}}. \quad (3.48)$$

Here, $S^{(k)}$ and $\tilde{O}^{(k)}(\alpha)$ stand for the values of operator S [Eq. (3.21)] and $\tilde{O}(\alpha)$ in Monte Carlo step k . Results of this computation are listed in the last column of Table III. As can be seen, the values for $\langle O(\alpha) \rangle$ so obtained are consistently slightly lower than those based on the pair wave function, with a slightly stronger dip at the origin than for the system described by the pair wave function.

Note that the values quoted for $\langle O(\alpha) \rangle$ correspond to a system of $N = 30$ particles occupying a disk of area $A' = \pi(N - \frac{1}{3})$, in contrast to the results for the Coulomb energy, where the contraction due to the quasiparticle is compensated.

D. States at $\nu = \frac{2}{5}$, $\frac{2}{3}$, and $\frac{2}{7}$

As a trial wave function for $\nu = \frac{2}{5}$, $\frac{2}{3}$, and $\frac{2}{7}$, we use pair wave functions $\psi = \alpha \tilde{\psi}$, (2.40), with $s = 2$, $u = t = 1$ for the $\frac{2}{5}$ state, $s = u = 1$, $t = 0$ for the $\frac{2}{3}$ state, and $s = 3$, $t = 0$, $u = 1$ for the $\frac{2}{7}$ state. As discussed in Sec. II, we hope that the antisymmetrizer α will produce only small corrections to the structure of the wave function and the Coulomb energy, and that its effect can be computed by perturbation methods. Let us therefore first ignore the

antisymmetrizer α . The probability density $|\tilde{\psi}|^2$ can be related to the statistical-mechanical problem defined by the Hamiltonian

$$\begin{aligned} \tilde{H} = & -2s \sum_{k < l} \ln |\mathbf{r}_k - \mathbf{r}_l| - 4u \sum_{i < j} \ln |\mathbf{R}_i - \mathbf{R}_j| \\ & + 2t \sum_i \ln |\mathbf{r}_{2i} - \mathbf{r}_{2i-1}| + \frac{2s+u}{2} \sum_k r_k^2. \end{aligned} \quad (3.49)$$

Here, k and l run from 1 to N , whereas i and j run up to $M = N/2$; \mathbf{R}_i is the center of mass position of pair $(2i-1, 2i)$. Note that length is measured in units of $R_0 = \sqrt{2s+u} l_0$.

1. Results before antisymmetrization

In Fig. 9 we show the radial distribution function for the $\nu = \frac{2}{5}$ state [Fig. 9(a)], the $\frac{2}{3}$ state [Fig. 9(b)], and the $\frac{2}{7}$ state [Fig. 9(c)], as obtained from Monte Carlo simulations based on Hamiltonian (3.49). The radial distribution function is computed via Eq. (3.3) with values $\Delta = \frac{1}{20}$ and $R_1 = 2R_0$ (implying that an average of $N_1 = 4$ particles contribute to the sum over j). In order to illustrate the finite-size effects, we show results for $g(r)$ in the $\nu = \frac{2}{5}$ state [Fig. 9(a)] for systems with $N = 72, 144$, and 196 particles. Notice the shoulderlike structure around $R = R_0$ and the shift of the peak of $g(R)$ from the usual value of $R \approx 1.8R_0$ to about $R \approx 2.5R_0$, which is larger by a factor of $\approx \sqrt{2}$, as would be expected if pairs are strongly bound. Notice also that the finite-size effects are negligible for $R \leq 2.5R_0$ for $N = 72$ and for $R \leq 6.5R_0$ for $N = 144$. Plots of $g(R)$ for the $\nu = \frac{2}{3}$ [Fig. 9(b)] and the $\nu = \frac{2}{7}$ state [Fig. 9(c)] are from simulations of systems with $N = 144$ particles. In contrast to the shape of $g(R)$ for the $\frac{2}{5}$ state, no conspicuous shoulderlike structure can be discerned on the rising part of the curve of $g(R)$ for the $\nu = \frac{2}{3}$ and $\frac{2}{7}$ states. This may be caused by the fact that, for $t = 0$, the repulsion of particles within the same pair is not decreased, as is the case in the $\frac{2}{5}$ state.

The Coulomb energy E/N for these nonantisymmetrized wave functions is listed in Table IV, together with the integral $C(R)$ [Eq. (3.4)]. Values for the thermodynamic limit are

from the Laughlin $\nu = \frac{1}{3}$ state via the electron-hole-symmetry relation,⁵

$$\nu u(\nu) = (1-\nu)u(1-\nu) + (\pi/8)^{1/2} \frac{e^2}{\epsilon l_0} (1-2\nu), \quad (3.51)$$

where $u(\nu)$ is the potential energy per electron in the state. This gives

$$E_L(\frac{2}{3})/N \approx -0.518e^2/\epsilon l_0, \quad (3.52)$$

which is somewhat higher than our result (3.50) for the nonantisymmetrized state.

Following Yoshioka,² let us now examine the asymptotic behavior of the radial distribution function $g(R)$ for small R . In Fig. 10 we show the asymptotic form of $g(R)$ by plotting $g(R)/R^2$ as a function of R^2 for both the $\nu = \frac{2}{5}$ (open circles) and the $\nu = \frac{2}{3}$ (plus signs) states. From this we deduce an asymptotic form

$$g(R) \sim c_1 R^2 + c_2 R^4 + O(R^6), \quad (3.53)$$

with

$$\tilde{c}_1 \approx \begin{cases} 1.3R_0^{-2} = 0.26l_0^{-3}, & \nu = \frac{2}{5} \\ 0.9R_0^{-2} = 0.3l_0^{-2}, & \nu = \frac{2}{3}, \end{cases} \quad (3.54)$$

and

$$\tilde{c}_2 \approx \begin{cases} -1.6R_0^{-4} = -0.064l_0^{-4}, & \nu = \frac{2}{5} \\ -0.17R_0^{-4} = -0.019l_0^{-4}, & \nu = \frac{2}{3}. \end{cases} \quad (3.55)$$

Again, the tilde denotes the fact that those values do not include antisymmetrization corrections. The corresponding values obtained by Yoshioka from exact numerical diagonalization of the Hamiltonian (using systems of up to eight particles) are

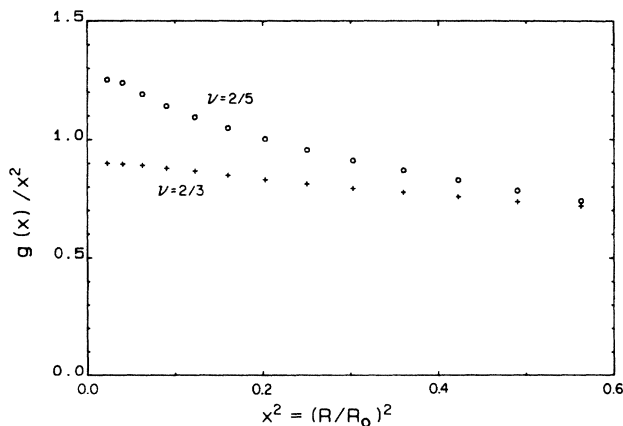


FIG. 10. Asymptotic behavior of radial distribution function $g(r)$ for small r . We plot $g(r)/r^2$ as a function of r^2 for the states $\nu = \frac{2}{5}$ (open circles) and $\nu = \frac{2}{3}$ (plus signs). Results are obtained using nonantisymmetrized pair wave function $\tilde{\psi}$, Eq. (2.40), with $s=2, t=u=1$ for $\nu = \frac{2}{5}$ and $s=u=1, t=0$ for $\nu = \frac{2}{3}$.

$$c_1^y \approx \begin{cases} 0.125l_0^{-2}, & \nu = \frac{2}{5} \\ 0.425l_0^{-2}, & \nu = \frac{2}{3} \end{cases} \quad (3.56)$$

and

$$c_2^y \approx \begin{cases} -0.03l_0^{-4}, & \nu = \frac{2}{5} \\ -0.10l_0^{-4}, & \nu = \frac{2}{3} \end{cases} \quad (3.57)$$

significantly different from our values \tilde{c}_n before antisymmetrization corrections are included.

2. Antisymmetrization

Let us now turn to the problem of calculating the effect of the antisymmetrizer a . The expectation value of any symmetric operator O in the fully antisymmetrized wave function can again be written as (cf. Sec. III C 2)

$$\langle O \rangle = \frac{\langle \psi | O | \psi \rangle}{\langle \psi | \psi \rangle} = \frac{\langle \tilde{\psi} | O a | \tilde{\psi} \rangle}{\langle \tilde{\psi} | a | \tilde{\psi} \rangle}. \quad (3.58)$$

In the case of the quasiparticle wave function (2.18), the antisymmetrizer consisted of, altogether, $O(N^2)$ permutations which could all be included in our numerical computation. However, in the present situation, although $\tilde{\psi}$ is already symmetric under arbitrary permutation of the pairs and antisymmetric with respect to interchanges of particles belonging to the same pair, the antisymmetrizer still consists of $O(M!)$ contributions, which for a sufficiently large system cannot all be included in a calculation. We thus have to resort to an approximate method. The basis of our approximation is to express the antisymmetrizer a in terms of particle exchange P_{ik} , where particles i and k belong to different pairs. We are guided here by the idea that, provided that the pairs had little overlap with one another, the effect of operator P_{ik} on the structure of the wave function would be small. Moreover, one would expect that products $P^{(n)}$ of n exchange operators, $P^{(n)} = P_{ik} P_{lm} \dots$, corresponding to many-particle interchanges, would have an effect which decreases with the order n as α^n , where α measures this overlap of different pairs.

If one expands the antisymmetrizer a to second order in P_{ik} , one finds

$$\begin{aligned} a &= 1 + a^{(1)} + a^{(2)} + a^{(3)} + O(P^{(3)}) \\ &= 1 - \sum'_{i,k} P_{ik} + \sum''_{i,k,l} P_{ik} P_{kl} + \sum'''_{i,k,l,m} P_{ik} P_{lm} + O(P^{(3)}). \end{aligned} \quad (3.59)$$

Denoting the number of pairs by M , the summation \sum' in (3.59) consists of, altogether, $M(M-1)$ terms; it can be written as

$$a^{(1)} = - \sum_{1 \leq i < k \leq M} (P_{2i,2k} + P_{2i,2k-1}). \quad (3.60)$$

Notice that $P_{2i-1,2k} \tilde{\psi} \equiv P_{2i,2k-1} \tilde{\psi}$ and $P_{2i-1,2k-1} \tilde{\psi} \equiv P_{2i,2k} \tilde{\psi}$ because of the symmetry of $\tilde{\psi}$ with respect to in-

terchange of pairs i and k . Therefore terms of the form $P_{2i-1, 2k}$ and $P_{2i-1, 2k-1}$ are implicitly included in summation (3.60). Note also that permutations $P_{2i, 2i-1}$ are not included in (3.54) since $\tilde{\psi}$ is already antisymmetric under their action. The second term $\alpha^{(2)}$ in Eq. (3.59) is the sum of $\frac{4}{3}M(M-1)(M-2)$ permutations involving cyclic interchange of three particles. Using the notation of cycles,

$$(i, k, l) \equiv P_{kl}P_{ik}, \quad (3.61)$$

it can be written as

$$\alpha^{(2)} = \sum_{\lambda, \kappa=0}^1 \sum_{i=1}^M \sum_{k>i}^M \sum_{\substack{l>i \\ l \neq k}}^M (2i, 2k-\kappa, 2l-\lambda). \quad (3.62)$$

Note that cycles in which the first element is odd are implicitly included in (3.62) because, when acting on $\tilde{\psi}$, permutations $(2i-1, 2k-\kappa, 2l-\lambda)$ are equivalent to $(2i, 2l-1+\lambda, 2k-1+\kappa)$.

Finally, the last term, $\alpha^{(3)}$, consists of $\frac{1}{2}M(M-1)(M-2)(M-3)$ permutations, each corresponding to two two-particle interchanges,

$$\alpha^{(3)} = \sum_{\kappa, \mu=0}^1 \sum_{i=1}^{M-3} \sum_{k>i}^M \sum_{\substack{l>i \\ l \neq k}}^{M-1} \sum_{\substack{m>l \\ m \neq k}}^M P_{2i, 2k-\kappa} P_{2l, 2m-\mu}. \quad (3.63)$$

Again, as in term $\alpha^{(1)}$, (3.60), permutations P , such as $P = P_{2i-1, 2k-\kappa} P_{2l-1, 2m-\mu}$, are implicitly included in Eq. (3.57) because of the symmetry properties of $\tilde{\psi}$.

With the use of expansion (3.59) for the antisymmetrizer α , the expectation value $\langle O \rangle$, Eq. (3.58), takes the form

$$\langle O \rangle = \frac{1}{D} \left[\langle\langle O \rangle\rangle + \sum_{n=1}^3 \langle\langle O \alpha^{(n)} \rangle\rangle \right] + O(P^{(3)}), \quad (3.64)$$

where

$$\langle\langle O \rangle\rangle \equiv \langle \tilde{\psi} | O | \tilde{\psi} \rangle / \langle \tilde{\psi} | \tilde{\psi} \rangle \quad (3.65)$$

and

$$D = 1 + \sum_{n=1}^3 \langle\langle \alpha^{(n)} \rangle\rangle + O(P^{(3)}). \quad (3.66)$$

For a symmetric operator, the first-order term can be written as [cf. Eq. (3.60)]

$$\langle\langle O \alpha^{(1)} \rangle\rangle = -M(M-1) \langle\langle OP_{13} \rangle\rangle, \quad (3.67)$$

while the two second-order terms, cf. (3.62) and (3.63), are given by

$$\langle\langle O \alpha^{(2)} \rangle\rangle = \frac{4}{3}M(M-1)(M-2) \langle\langle OP_{13}P_{35} \rangle\rangle \quad (3.68)$$

and

$$\langle\langle O \alpha^{(3)} \rangle\rangle = \frac{1}{2}M(M-1)(M-2)(M-3) \langle\langle OP_{13}P_{57} \rangle\rangle. \quad (3.69)$$

The calculation of expectation value $\langle\langle OP \rangle\rangle$ for any permutation P is done by Monte Carlo importance sampling using the procedure outlined in Sec. III C 2. Again, $\tilde{\psi}^* P \tilde{\psi}$ is expressed as $R_P |\tilde{\psi}|^2$, where $R_P = P \tilde{\psi} / \tilde{\psi}$ is the ratio of two polynomials, and the updating of configura-

tions is controlled by Hamiltonian \tilde{H} [Eq. (3.49)]. A problem arises, however, with the expansion of expectation value $\langle O \rangle$ in the form of Eqs. (3.64) and (3.66). This becomes obvious if we examine the first-order correction, Eq. (3.67), for instance, for the case $O \equiv 1$, as occurs in the denominator D , (3.66). We would expect that the contributions to expectation value $\langle\langle P_{13} \rangle\rangle$ will mainly originate from regions in phase space in which the separation of particles 1 and 3 is less than the correlation length ξ of the system. Since the probability that particle 3 will lie within a disk of radius ξ around particle 1 is $O(\xi^2/N)$, we expect that

$$\langle\langle \alpha^{(1)} \rangle\rangle \sim O(\xi^2 N), \quad (3.70)$$

which implies that even for very small overlap of different pairs, as the number of pairs M increases, the first-order "correction" will exceed the "leading" contribution, unity, in (3.66). The same argument will, of course, also apply to the numerator in Eq. (3.64). This suggests that one should formulate the expansion in powers of P_{ik} for the ratio directly. Expanding D^{-1} [Eq. (3.64)] up to second order in P_{ik} , we obtain

$$\begin{aligned} \langle O \rangle &= \langle\langle O \rangle\rangle + \sum_{n=1}^3 \{ \langle\langle O \alpha^{(n)} \rangle\rangle - \langle\langle O \rangle\rangle \langle\langle \alpha^{(n)} \rangle\rangle \} \\ &\quad - \langle\langle \alpha^{(1)} \rangle\rangle [\langle\langle O \alpha^{(1)} \rangle\rangle - \langle\langle O \rangle\rangle \langle\langle \alpha^{(1)} \rangle\rangle] + O(P^{(3)}), \end{aligned} \quad (3.71)$$

which is in effect a linked-cluster expansion.^{23,24}

Indeed, using expressions (3.67)–(3.69) for $\langle\langle O \alpha^{(n)} \rangle\rangle$, we find

$$\langle O \rangle + \langle\langle O \rangle\rangle + \sum_{n=1}^3 \Delta_0^{(n)} + O(P^{(3)}), \quad (3.72)$$

with the first-order correction

$$\Delta_0^{(1)} = -M(M-1) \langle\langle OP_{13} \rangle\rangle_c \quad (3.73)$$

and two second-order corrections, one due to cyclic three-particle exchanges

$$\begin{aligned} \Delta_0^{(2)} &= \frac{4}{3}M(M-1)(M-2) [\langle\langle OP_{13}P_{35} \rangle\rangle \\ &\quad - \langle\langle O \rangle\rangle \langle\langle P_{13}P_{35} \rangle\rangle] \\ &\quad - M(M-1)(4M-6) \langle\langle P_{13} \rangle\rangle \langle\langle OP_{13} \rangle\rangle_c, \end{aligned} \quad (3.74)$$

and the other due to (pairwise) four-particle interchanges

$$\Delta_0^{(3)} = \frac{1}{2}M(M-1)(M-2)(M-3) \langle\langle OP_{13}P_{57} \rangle\rangle_c. \quad (3.75)$$

We have used cumulant notation,

$$\langle\langle AB \rangle\rangle_c = \langle\langle AB \rangle\rangle - \langle\langle A \rangle\rangle \langle\langle B \rangle\rangle \quad (3.76)$$

and

$$\begin{aligned} \langle\langle ABC \rangle\rangle_c &= \langle\langle ABC \rangle\rangle - \langle\langle AB \rangle\rangle \langle\langle C \rangle\rangle \\ &\quad - \langle\langle AC \rangle\rangle \langle\langle B \rangle\rangle - \langle\langle BC \rangle\rangle \langle\langle A \rangle\rangle \\ &\quad + 2 \langle\langle A \rangle\rangle \langle\langle B \rangle\rangle \langle\langle C \rangle\rangle, \end{aligned} \quad (3.77)$$

for arbitrary operators A , B , and C .

Here we have split the last term of Eq. (3.71), $-M^2(M-1)^2\langle\langle P_{13}\rangle\rangle\langle\langle OP_{13}\rangle\rangle_c$, in a somewhat arbitrary manner into two parts, one included in cumulant $\langle\langle OP_{13}P_{57}\rangle\rangle_c$ in correction $\Delta^{(3)}$ [Eq. (3.75)] and the remainder taken into account in $\Delta^{(2)}$ [Eq. (3.74)]. We have not used cumulant notation (3.77) for the contribution due to permutation $P_{13}P_{35}$ in Eq. (3.74) since the factorization of cyclic permutation (153) into two two-particle exchanges is not fundamental and it would be more natural to define the cumulant by the expression in square brackets in Eq. (3.74).

In the following we will also make use of the definition of the fractional change,

$$R_O^{(i)} = \Delta_O^{(i)} / \langle\langle O \rangle\rangle, \quad (3.78)$$

of the expectation value $\langle O \rangle$ of operator O due to the contribution $\alpha^{(i)}$ to the antisymmetrizer α , writing

$$\langle O \rangle = \langle\langle O \rangle\rangle \left[1 + \sum_{i=1}^3 R_O^{(i)} + O(P^3) \right]. \quad (3.79)$$

Let us now turn to the results of computations of antisymmetrization corrections. In Fig. 11 we show the behavior of the expectation value $\langle\langle \alpha^{(1)} \rangle\rangle$ of the first-order contribution to the antisymmetrizer α as a function of the number of particles N . Crosses represent values of $\langle\langle \alpha^{(1)} \rangle\rangle$ for the $\nu = \frac{2}{3}$ state and diamonds those for $\nu = \frac{2}{5}$. The size of the vertical bars indicate the standard deviation. Results are from simulations with between 100 000 and 600 000 Monte Carlo configurations. Consistent with our discussion above [cf. Eq. (3.70)], $\langle\langle \alpha^{(1)} \rangle\rangle$ increases linearly with N . (We note that plotting $[M/(M-1)]\langle\langle \alpha^{(1)} \rangle\rangle$ instead of $\langle\langle \alpha^{(1)} \rangle\rangle$ [cf. (3.67)] results in a behavior accurately fitted by a straight line through the origin.) We also note that the expectation value has a different sign for the states $\nu = \frac{2}{5}$ and $\frac{2}{3}$ and is about 5 times larger in absolute value for the latter.

Let us now turn to the effects of antisymmetrizer α on

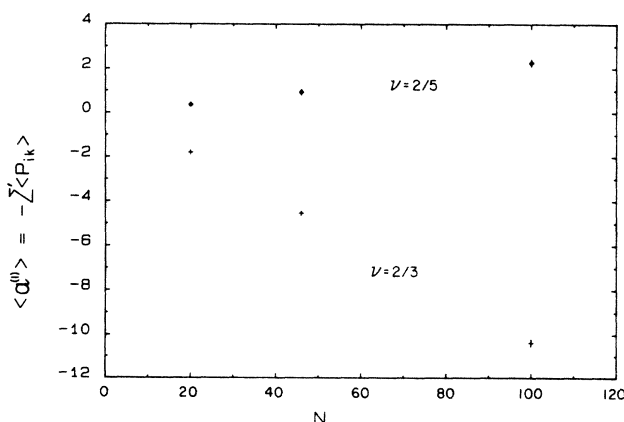


FIG. 11. Expectation value $\langle\langle \alpha^{(1)} \rangle\rangle = -\sum' \langle\langle P_{ik} \rangle\rangle$, Eq. (3.60), of the first-order contribution $\alpha^{(1)}$ to the antisymmetrizer α . Shown are Monte Carlo results for the $\nu = \frac{2}{5}$ and $\frac{2}{3}$ states. For definition of wave functions, cf. Figs. 9 and 10. The length of the vertical bars denotes the statistical error.

the Coulomb energy. In Fig. 12 we plot results for the fractional change $R_E^{(1)} = \Delta_E^{(1)} / \tilde{E}$ caused by two-particle exchanges $\alpha^{(1)}$ as a function of system size ($1/N$) for the states $\nu = \frac{2}{5}$ (circles), $\nu = \frac{2}{7}$ (triangles), and $\nu = \frac{2}{3}$ (squares). Systems with $N = 20, 46$, and 100 particles are used. In all three cases, the dependence on $R_E^{(1)}$ on system size is very weak and an accurate determination of its behavior as a function of $1/N$ would require much smaller statistical errors. However, data are consistent with the following values, for $N = \infty$:

$$R_E^{(1)} \approx \begin{cases} 0.010 \pm 0.003, & \nu = \frac{2}{5} \\ -0.007 \pm 0.002, & \nu = \frac{2}{7} \\ -0.030 \pm 0.006, & \nu = \frac{2}{3}. \end{cases} \quad (3.80)$$

As we can see, the effect of two-particle exchanges results in a lowering of the energy for the $\nu = \frac{2}{5}$ state, but an increase for the states $\nu = \frac{2}{7}$ and $\frac{2}{3}$. Including these shifts, we find energies

$$\frac{E^{(1)}}{N} = \frac{\tilde{E}}{N} (1 + R_E^{(1)}) \approx \begin{cases} -0.414(2), & \nu = \frac{2}{5} \\ -0.377(2), & \nu = \frac{2}{7} \\ -0.502(2), & \nu = \frac{2}{3}. \end{cases} \quad (3.81)$$

In Table V we list the results of computations with $N = 20$ particles of the higher-order contributions $R_E^{(2)}$ and $R_E^{(3)}$ owing to the effects of the three- and four-particle exchanges $\alpha^{(2)}$ and $\alpha^{(3)}$. We note that neither for the $\nu = \frac{2}{5}$ nor the $\nu = \frac{2}{7}$ state do statistically significant contributions to the energy result, while for the $\nu = \frac{2}{3}$ state a small additional contribution about 5 times smaller in magnitude and of opposite sign from the leading contribution $R_E^{(1)}$ is obtained. Assuming that finite-size effects are unimportant, we obtain values for the energy

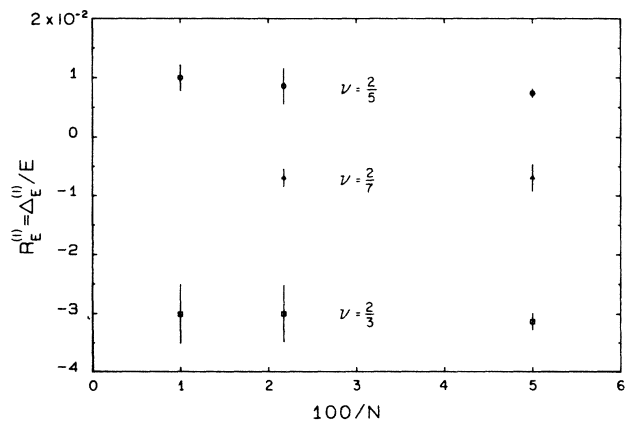


FIG. 12. Antisymmetrization corrections to Coulomb energy E . Shown are Monte Carlo results for the correction $R_E^{(1)} = \Delta_E^{(1)} / E$, Eqs. (3.73), due to two-particle interchanges for the states $\nu = \frac{2}{5}$ (open circles), $\nu = \frac{2}{3}$ (squares), and $\nu = \frac{2}{7}$ (triangles). Results are plotted for systems with $N = 20, 46$, and 100 electrons as a function of N^{-1} .

TABLE V. Antisymmetrization corrections to energy of the $\nu = \frac{2}{5}$, $\frac{2}{3}$, and $\frac{2}{7}$ states. Listed are Monte Carlo results for the fractional change $R_E^{(i)}$ [Eqs. (3.73)–(3.78)] of the Coulomb energy due to two-particle interchanges $\alpha^{(1)}$, cyclic three-particle interchanges $\alpha^{(2)}$, and two two-particle interchanges $\alpha^{(3)}$ [cf. Eqs. (3.60)–(3.63)]. Systems with 20 electrons are used. Consult Table IV for definitions of wave functions.

Operator	$\nu = \frac{2}{5}$	R_E $\nu = \frac{2}{7}$	$\nu = \frac{2}{3}$
$\alpha^{(1)} = \sum' P_{ik}$	+0.0074(7)	-0.0065(7)	-0.031(1)
$\alpha^{(2)} = \sum'' P_{ik} P_{kl}$	-0.0001(16)	+0.0005(30)	+0.005(6)
$\alpha^{(3)} = \sum''' P_{ik} P_{lm}$	+0.0002(10)	+0.0005(27)	+0.001(6)
Total	+0.0075(20)	-0.0055(41)	-0.025(9)

including antisymmetrization corrections up to $O(P^2)$,

$$E^{(2)} \approx \begin{cases} -0.414(2), & \nu = \frac{2}{3} \\ -0.377(3), & \nu = \frac{2}{7} \\ -0.509(5), & \nu = \frac{2}{5}. \end{cases} \quad (3.82)$$

These results should be compared to those obtained by Yoshioka by exact numerical diagonalization of systems with up to $N=6$ particles (using a rectangular cell with periodic boundary conditions). His value for the $\nu = \frac{2}{5}$ state, $E/N \approx -0.435$, is so significantly lower that the difference cannot be attributed to finite-size effects and it appears that our pair wave function (2.39) for $s=2$, $u=t=1$ is *not* a good trial wave function for this state. It is interesting to note that the value $\tilde{E}/N \approx -0.410$ [Eq. (3.50)] corresponds reasonably well to the value $E/N \approx -0.409$ that one would obtain from Eq. (1.2), constructing the $\nu = \frac{2}{5}$ state by adding quasiparticles to the $\nu = \frac{1}{3}$ state, and using for $\tilde{\epsilon}_+(\frac{1}{3})$ the value $\tilde{\epsilon}_+^{(0)} \approx 0.103$ (Table II) based on the *nonantisymmetrized* pair wave function $\tilde{\psi}_0^{(+)}$ [Eq. (2.19)] for the quasiparticle. By contrast, the value $E/N \approx -0.424$ is obtained from Eq. (1.2) if one uses the value $\tilde{\epsilon}_+ \approx 0.073$ obtained from the properly antisymmetrized quasiparticle wave function. One might have hoped that the antisymmetrization corrections would decrease the energy of the $\nu = \frac{2}{5}$ state accordingly. Up to order P^2 , however, the antisymmetrization corrections do not achieve this. We cannot completely rule out the possibility that the fully antisymmetrized wave function $\psi = \alpha\tilde{\psi}$ [Eq. (2.38)] would have a significantly lower energy, but this seems unlikely in view of the smallness of the $O(P^2)$ correction obtained above.

The result $E^{(2)}/N \approx -0.377$ for the $\nu = \frac{2}{7}$ state may look more promising: the value obtained by Yoshioka is $E/N \approx -0.385$ for $N=4$, and differs from our value by a similar amount as in the case of the $\nu = \frac{1}{3}$ state (for which $E^y \approx -0.416$, compared to the energy of the Laughlin state, $E/N \approx -0.410$). However, we should bear in mind that at low filling fractions the difference between the ground-state energy and the classical plasma energy gets very small ($E_{\text{classical}}/N \approx -0.3838$ at $\nu = \frac{2}{7}$, cf. Ref. 13), so that the accuracy required for a calculation to be useful becomes accordingly great.

As expected, our values for the energy of the antisymmetrized $\nu = \frac{2}{3}$ state $E^{(2)}/N \approx -0.509$, is higher than the value $E_L/N = -0.518$ obtained using particle-hole symmetry, according to Eqs. (3.51)–(3.52), and the energy at the Laughlin wave function for $\nu = \frac{1}{3}$.²⁵ This shows that our pair wave function (2.39), with $s=1$, $u=1$, $t=0$, is not as good a trial wave function as the wave function obtained by particle-hole duality from Laughlin's $\nu = \frac{1}{3}$ state.

3. Radial distribution function near $r=0$

Let us now turn to the asymptotic behavior of the radial distribution function. In order to study the effects of the antisymmetrizer on its form, we compute antisymmetrization corrections to Gaussian integrals,

$$G_\mu = 2\mu^2 \int g(r) e^{-\mu r^2} r dr, \quad (3.83)$$

which can be computed also from

$$G_\mu = \langle O_\mu \rangle = \frac{2\mu^2}{N} \sum_{i < j} e^{-\mu(\tau_i - \tau_j)^2}, \quad (3.84)$$

and which, for large values of μ , will tend to c_1 [Eq. (3.53)]. In Table VI we list results for the fractional change $R_\mu^{(i)}$ to the expectation value $\langle O_\mu \rangle$ resulting from two-, three-, and four-particle interchanges $\alpha^{(1)}$, $\alpha^{(2)}$, and $\alpha^{(3)}$, both for the $\nu = \frac{2}{3}$ and the $\nu = \frac{2}{5}$ state.

Systems with 20 particles are used and results are from 400 000 and 600 000 Monte Carlo configurations. As can be seen, the major contribution does come from two-particle exchanges, in both systems. However, for the $\nu = \frac{2}{3}$ state a statistically significant contribution also comes from cyclic three-particle interchanges $\alpha^{(2)}$, whose effect is about 4–5 times smaller than the leading contribution, $R_\mu^{(1)}$. Performing an extrapolation to $\mu = \infty$, we obtain

$$R_{\mu=\infty} \approx 0.43 \pm 0.15, \quad \nu = \frac{2}{3} \quad (3.85)$$

and using $\tilde{c}_1 \approx 0.3l_0^{-2}$.

$$c_1 \approx (0.43 \pm 0.05)l_0^{-2}, \quad \nu = \frac{2}{3} \quad (3.86)$$

consistent with the value obtained by Yoshioka.

For the $\nu = \frac{2}{5}$ state, results for the higher-order corrections are very noisy and no reliable extrapolation to $\mu = \infty$

TABLE VI. Antisymmetrization corrections to short-range behavior of radial distribution function for the $\nu = \frac{2}{3}$ and $\frac{2}{5}$ states. Listed are the Monte Carlo results for the fractional change $R_\mu^{(i)}$ Eq. (3.78), to the Gaussian-weighted integral G_μ , Eq. (3.83), of the radial distribution function $g(r)$. The definition of wave functions same as for Tables IV and V.

	$\nu = \frac{2}{3}$			$\nu = \frac{2}{5}$		
	$\mu = 2.77$	$\mu = 5.55$	$\mu = 11.1$	$\mu = 2.77$	$\mu = 5.55$	$\mu = 11.1$
$R_\mu^{(1)}$	0.197(7)	0.257(13)	0.297(26)	-0.064(4)	-0.080(8)	-0.083(15)
$R_\mu^{(2)}$	0.046(19)	0.063(38)	0.078(65)	-0.001(15)	0.004(29)	0.018(44)
$R_\mu^{(3)}$	0.013(25)	0.009(46)	-0.015(86)	-0.007(6)	-0.006(10)	-0.004(17)
$R_\mu = \sum R_\mu^{(i)}$	0.256(32)	0.329(61)	0.360(110)	-0.072(17)	-0.082(32)	-0.069(50)

is possible. In any case, including two-, three-, and four-particle interchanges $\alpha^{(1)}$, $\alpha^{(2)}$, and $\alpha^{(3)}$ will not lead to a decrease in c_1 by more than about 15%, leading to a value $c_1 \approx 0.22l_0^{-2}$, still very significantly larger than Yoshioka's results $c_1^y \approx 0.125l_0^{-2}$. This again points to a serious problem with our trial wave function, in the case $\nu = \frac{2}{5}$.

ACKNOWLEDGMENTS

The authors are grateful for conversations with many colleagues on the subject of this paper, including R. B. Laughlin, F. D. M. Haldane, P. M. Platzman, S. M. Girvin, H. Fertig, C. Kallin, and H. L. Stormer. The work at Harvard University was supported in part by National Science Foundation Grant No. DMR-82-07431.

APPENDIX A: APPROXIMATE RELATION BETWEEN ENERGY OF $\nu = \frac{2}{3}$

STATE AND QUASIPARTICLE ENERGY AT $\nu = \frac{1}{3}$

In Ref. 8 an approximate iterative formula was developed for the ground-state and elementary excitation energies of the quantized Hall states, based on the hierarchical construction. Here, we shall restate this approximate formula, and illustrate its use in deriving the relation between $E(\frac{2}{3})$ and $\tilde{\epsilon}_+(\frac{1}{3})$, quoted in Eq. (1.2) above.

According to the hierarchical construction, each stable quantized Hall state is represented uniquely by a finite sequence^{6,8} of the form

$$(p_1, \alpha_1, p_2, \alpha_2, \dots, p_s, \alpha_s),$$

where p_r is a positive integer, and $\alpha_r = \pm 1$. Among the essential parameters of the quantized Hall state, determined by the sequence, are the filling factor ν_s , the charge $q_s e$ of the elementary "particlelike" excitation, and a rational number m_s , which characterizes the fractional statistics of the quasiparticles.

If a sequence of length s is extended by addition of an integer p_{s+1} and a sign α_{s+1} , we obtain a new sequence, characterizing a state with filling factor ν_{s+1} , which we say is *derived* from the previous state ν_s . The parameters of the state at level $s+1$ are related to those of the parent state by

$$m_{s+1} = 2p_{s+1} - \alpha_{s+1} / m_s, \quad (\text{A1})$$

$$\nu_{s+1} = \nu_s + \alpha_{s+1} q_s / |q_s| / m_{s+1}, \quad (\text{A2})$$

$$q_{s+1} = \alpha_{s+1} q_s / m_{s+1}. \quad (\text{A3})$$

As starting values for these parameters, we set $\nu_0 = 0$, and $q_0 = m_0 = \alpha_1 = 1$.

The approximate energy formula is obtained by assuming that at any stage of the hierarchy the quasiparticles or quasiholes can be treated as point particles of charge $\pm q_s e$, and that the derived state ν_{s+1} can be represented accurately by placing the appropriate number of quasiparticles in a Laughlin pair wave function, appropriate to the fractional statistics of the quasiparticles. Because the potential energy of the Laughlin state is determined by the pair-correlation function of a classical one-component plasma, one can then derive the approximate relation

$$E(\nu_{s+1}) \cong E(\nu_s) + n_s \epsilon_\pm(\nu_s) + n_s |q_s|^{5/2} u_{pl}(m_{s+1}), \quad (\text{A4})$$

where $E(\nu)$ is the energy per quantum of magnetic flux, $n_s \equiv |q_s| / m_{s+1}$ is the density of quasiparticles in the Laughlin wave function, measured in units of $|2\pi Be / \hbar c|$, and $\epsilon_\pm(\nu_s)$ is the gross energy of a single quasiparticle or quasihole. The function $u_{pl}(m_{s+1})$ is the potential energy per particle, in units of $e^2 / \epsilon l_0$, for a set of particles of charge e , obtained from the pair-correlation function of a classical one-component plasma, at plasma parameter $\Gamma = 2m_{s+1}$. (The plasma parameter is a dimensionless measure of the inverse temperature of the plasma.) The factor $|q_s|^{5/2}$ reflects the smaller charge and larger magnetic length of the quasiparticles. We note that the argument of u_{pl} was incorrectly stated as m_s , in Ref. 8. The quantity u_{pl} is clearly a smooth function of its argument, and various analytic formulas have been proposed to interpolate between points which have been fixed by Monte Carlo evaluations.^{3,8,13}

In order to use the approximate energy formula, it is necessary to adjoin a suitable approximation for the quasiparticle or quasihole energy $\epsilon_\pm(\nu_s)$. Using the Laughlin wave function for a quasihole excitation, one can express the energy $\epsilon_-(\nu_s)$ in terms of the previous quasiparticle or quasihole energy $\epsilon_+(\nu_{s-1})$ and the quasihole energy for the Laughlin state at plasma parameter $\Gamma = 2m_s$, for which a reasonably accurate formula exists. [See Eqs. (9)

and (10) of Ref. 8.] For the quasiparticle energy, however, the situation has been much less clear, and it was necessary in Ref. 8 to adopt a crude approximation—for purposes of illustration, it was assumed that the proper energy of a quasiparticle is simply 3 times the proper quasi-hole energy at the same value of ν .

In the present paper we wish to use Eq. (A4) to estimate the energy per electron of the $\nu = \frac{2}{3}$ state, based on our new Monte Carlo evaluations of the proper quasiparticle energy $\tilde{\epsilon}_+(\frac{1}{3})$ at the parent state $\nu = \frac{1}{3}$.

The state $\nu = \frac{1}{3}$ is described by a sequence of length $s = 1$, with $p_1 = 2$, $\alpha_1 = 1$. The state $\nu = \frac{2}{3}$ has $s = 2$, with the additional parameters $p_2 = 1$ and $\alpha_2 = 1$. From formulas (A1)–(A3), we see that $m_1 = 3$, $q_1 = \frac{1}{3}$, $m_2 = \frac{5}{3}$, and $n_1 = \frac{1}{5}$. Since $E(\frac{1}{3}) \cong \frac{1}{3}u_{pl}(3)$, we have, from (A4),

$$E(\frac{2}{3}) \cong \frac{1}{5}\epsilon_+(\frac{1}{3}) + \frac{1}{3}u_{pl}(3) + \frac{1}{5}(\frac{1}{3})^{5/2}u_{pl}(\frac{5}{3}). \quad (\text{A5})$$

From Eq. (2.25) above, or from Eq. (9) of Ref. 8, we have

$$\epsilon_+(\frac{1}{3}) \cong \tilde{\epsilon}_+(\frac{1}{3}) + \frac{1}{2}u_{pl}(3). \quad (\text{A6})$$

Thus, dividing both sides of (A5) by $\nu_2 = \frac{2}{3}$, we obtain the energy per particle, in the form of Eq. (1.2), as $A + \frac{1}{2}\tilde{\epsilon}_+(\frac{1}{3})$, where

$$A = \frac{13}{12}u_{pl}(3) + \frac{1}{2}(\frac{1}{3})^{5/2}u_{pl}(\frac{5}{3}). \quad (\text{A7})$$

The numerical value $A = -0.461$ is obtained from the result $u_{pl}(3) = -0.410$, derived in Sec. III A above, and the Monte Carlo result $u_{pl}(\frac{5}{3}) = -0.520$, which we have obtained by the same method as $u_{pl}(3)$.

APPENDIX B: COMPUTATIONAL METHOD FOR ARRAY PROCESSORS

1. Efficient Monte Carlo simulation

Like most array processors, the CSPI MAP-300 used for our computations is programmed by calls to special subroutines performing arithmetic operations on vectors or matrices, such as producing the sum $u_i + v_i$ of two vectors u_i and v_i , the logarithmic $\log_{10}u_i$ of all elements, etc. No matter how an array processor is constructed, each call of such subroutine involves a certain overhead, independent of the vector dimension. In the MAP-300 this overhead amounts to a minimum of about a thousand

floating point multiplications (or, since, in parallel with these, 2000 additions can take place, a total of about 3000 floating point operations). For this reason, efficient use of the array processor is only possible if each subroutine call involves many thousand floating point operations. This is not easy to achieve in the usual Metropolis Monte Carlo algorithm in which only one or a small fraction of all particles are moved at once, unless very large systems (with $N \sim 1000$ particles or larger) are used. The method we use in the present work consists of performing independent Monte Carlo computations on many systems in parallel.

The number N_S of independent systems is chosen such that $NN_S \sim 2000$, where N is the number of particles in each system. For each Monte Carlo step, in each system k one particle is chosen at random, it is moved by a random amount $\Delta r^{(k)}$, the change in energy $\Delta E^{(k)}$ is computed and the move is accepted if $\exp(-\Delta E^{(k)}) > u^{(k)}$, ($u^{(k)}$ being a uniformly distributed random number between zero and one), and otherwise rejected. This process is carried out for all N_S systems in parallel and thus the overhead is shared by N_S independent Monte Carlo computations and can be made negligible. The whole computation is carried out in the MAP, without host interference (Hewlett-Packard HP-1000/E) since the MAP contains its own manager system, which allows decisions to be made, loop control and the initiation of data and command transfers from or to the host. In this mode of operation the host is used exclusively for storing programs into the MAP and retrieving results from the MAP for further analysis and storage on magnetic disk.

2. Computation of antisymmetrization corrections

In this subsection we sketch our method for computing antisymmetrization corrections using the example of the two-particle exchange operator $\alpha^{(1)}$ [Eq. (3.60)] and pair wave function $\tilde{\psi}$ [Eq. (2.39)]. As discussed in detail in Sec. III, we need to compute the sum of the ratios

$$R_{lm}[z_i] = P_{lm}\tilde{\psi}[z_i]/\tilde{\psi}[z_i]$$

[cf. Eqs. (3.37) and (3.38)], which is the ratio of two polynomials. Using the notation

$$z_i^{(1)} \equiv z_{2i-1}, \quad z_i^{(2)} \equiv z_{2i}, \quad Z_i \equiv z_i^{(1)} + z_i^{(2)},$$

the ratio $R_{2l,2m}$ takes the form

$$R_{2l,2m}[z_i] = P_{2l,2m}\tilde{\psi}/\tilde{\psi} \\ = (-1)^s \left[\frac{(z_l^{(1)} - z_m^{(2)})(z_l^{(2)} - z_m^{(1)})}{(z_l^{(1)} - z_l^{(2)})(z_m^{(1)} - z_m^{(2)})} \right]^{-t} \left[\frac{z_l^{(1)} + z_m^{(2)} - (z_l^{(2)} + z_m^{(1)})}{Z_l - Z_m} \prod_{\substack{i \neq l \\ i \neq m}} \frac{(z_l^{(1)} + z_m^{(2)} - Z_i)(z_l^{(2)} + z_m^{(1)} - Z_i)}{(Z_l - Z_i)(Z_m - Z_i)} \right]^{2u}, \quad (\text{B1})$$

and similarly for $R_{2l-1,2m}$. This can be further simplified if we introduce the quantities

$$S_{ik}(l,m) = \prod_{n \neq l,m} (z_i^{(i)} + z_m^{(k)} - Z_n) \quad (\text{B2})$$

for $1 \leq l < m \leq M = N/2$ and $i, k = 1, 2$, and

$$T(l) = \prod_{n \neq l} (Z_l - Z_n) \quad (\text{B3})$$

for $1 \leq l \leq M = N/2$.

The ratio $R_{2l,2m}$ then reads

$$R_{2l,2m}[z_i] = (-1)^s \left[\frac{(z_l^{(1)} - z_m^{(2)})(z_l^{(2)} - z_m^{(1)})}{(z_l^{(1)} - z_l^{(2)})(z_m^{(1)} - z_m^{(2)})} \right]^{-t} \left[\frac{S_{12}(l,m)S_{21}(l,m)}{T(l)T(m)} [z_l^{(1)} + z_m^{(2)} - (z_l^{(2)} + z_m^{(1)})](Z_l - Z_m) \right]^{2u}, \quad (\text{B4})$$

and equivalently for ratio $R_{2l-1,2m}$. The most efficient computation results if these ratios are computed for all exchange operators $P_{2l,2m}$ and $P_{2l-1,2m}$ ($1 \leq l < m \leq M = N/2$) in parallel, i.e., vectorizing in l, m . The computation thus proceeds by first calculating $S_{ik}(l, m)$ for all values of l, m as well as the quantities $T(l)$. This is done by forming vectors such as $V_1(l, m) = z_l^{(i)} + z_m^{(k)} - Z_1$ (vector in l, m), $V_2(l, m) = z_l^{(i)} + z_m^{(k)} - Z_2$, and before computing the product $V_1 V_2$ to replace the values $z_l^{(i)} + z_m^{(k)} - Z_1$ for $l=1$ or $m=1$ and $z_l^{(i)} + z_m^{(k)} - Z_2$ for $l=2$ or $m=2$ by unity. This is done using a table which, for each value of the running index n , lists the elements of the corresponding vectors to be replaced by unity. Thereby the conditions in $n \neq l, m$ is removed from the loops. In the MAP-300 this replacement is carried out by the "manager processor" (called CSPU) in parallel with the arithmetic processor (while the product $V_1 V_2$ is computed using the arithmetic processor, the "ones" are put into V_3 by the CSPU). The remainder of the computation, according to Eq. (B4), is straightforward.

Equations similar to (B4) can be derived for three- and four-particle exchanges (ijk) and $(ij)(kl)$ [cf. Eqs. (3.61)–(3.63)], expressing the corresponding ratios in

terms of $S_{nm}(i, j)$ and $T(i)$. Again, high efficiency on the array processor is achieved by vectorizing over all exchange contributions (ijk) and $(ij)(kl)$, respectively.

3. Random number generators

The generation of pseudorandom numbers is done in the "manager" processor (CSPU) of the MAP-300 array processor, using the Tausworthe algorithm,²⁶ as discussed in detail by Kirkpatrick and Stoll,²⁷

$$I_n = \text{XOR}(I_{n-250}, I_{n-103}), \quad (\text{B5})$$

where XOR is the exclusive-or and I_n are, in our case, 16-bit (binary digit) integers. Initial 250-seed integers are generated using a standard random number generator (of the power-residue type) to generate 250 "random" bits, and then the Tausworthe algorithm (B5) is used to generate the 4000 bits ($= 250 \times 16$ bits) for the seed numbers.

Uniformly and Gaussian distributed pseudorandom numbers are generated from these 16-bit integers in the standard way, by first converting them into suitable floating point numbers and summing an appropriate number to obtain Gaussian statistics.

- ¹See, for example, D. C. Tsui, H. L. Störmer, and A. C. Gossard, *Phys. Rev. Lett.* **48**, 1559 (1982); H. L. Störmer, A. M. Chang, D. C. Tsui, J. C. M. Hwang, A. C. Gossard, and W. Wiegmann, *ibid.* **50**, 1953 (1983); A. M. Chang, P. Berglund, D. C. Tsui, H. L. Störmer, and J. C. M. Hwang, *Phys. Rev. Lett.* **53**, 997 (1984); E. E. Mendez, L. L. Chang, M. Heiblum, L. Esaki, M. Naughton, K. Martin, and J. Brooks, *Phys. Rev. B* **30**, 7310 (1984), and references therein.
- ²D. Yoshioka, B. I. Halperin, and P. A. Lee, *Phys. Rev. Lett.* **50**, 1219 (1983); *Surf. Sci.* **142**, 155 (1984); D. Yoshioka, *Phys. Rev. B* **29**, 6833 (1984).
- ³R. B. Laughlin, *Phys. Rev. Lett.* **50**, 1395 (1983).
- ⁴B. I. Halperin, *Helv. Phys. Acta* **56**, 75 (1983).
- ⁵See, for example, H. Fukuyama, P. M. Platzman, and P. W. Anderson, *Phys. Rev. B* **19**, 5211 (1979); D. Yoshioka, *ibid.* **29**, 6833 (1984); S. M. Girvin, *ibid.* **29**, 6012 (1984).
- ⁶F. D. M. Haldane, *Phys. Rev. Lett.* **51**, 605 (1983).
- ⁷R. B. Laughlin, *Surf. Sci.* **142**, 163 (1984).
- ⁸B. I. Halperin, *Phys. Rev. Lett.* **52**, 1583 (1984); **52**, 2390(E) (1984).
- ⁹T. Chakraborty, *Phys. Rev. B* **31**, 4026 (1985).
- ¹⁰S. M. Girvin, A. H. MacDonald, and P. M. Platzman, *Phys. Rev. Lett.* **54**, 581 (1985).
- ¹¹F. D. M. Haldane and E. H. Rezayi, *Phys. Rev. Lett.* **54**, 237 (1985).
- ¹²See, for example, A. M. Chang, M. A. Paalanen, D. C. Tsui, H. L. Störmer, and J. C. M. Hwang, *Phys. Rev. B* **28**, 6133 (1984); S. Kawaji, J. Wakabayashi, J. Yoshino, and H. Sasaki, *J. Phys. Soc. Jpn.* **53**, 1915 (1984); J. Wakabayashi, S. Kawaji, J. Yoshino, and H. Sasaki, (unpublished); G. Ebert, K. V.

Klitzing, J. C. Maan, G. Remenyi, C. Probst, G. Weimann, and W. Schlapp, *J. Phys. C* **17**, L775 (1984); J. Ihm and J. C. Phillips (unpublished).

¹³D. Levesque, J. J. Weis, and A. H. MacDonald, *Phys. Rev. B* **30**, 1056 (1984).

¹⁴S. T. Chui, T. Hakim, and K. B. Ma (unpublished).

¹⁵S. T. Chui, *Phys. Rev. B* **32**, 1436 (1985).

¹⁶Strictly speaking, the strong-field limit is violated at short separations. However, the corrections arising from the admixture of states from higher Landau levels are small. Moreover, the Coulomb repulsion is softened at short distance due to the finite thickness of the electron layer. Compare D. Yoshioka, *J. Phys. Soc. Jpn.* **53**, 3740 (1984); A. H. MacDonald, *Phys. Rev. B* **30**, 4392 (1984); A. H. MacDonald and G. C. Aers, *ibid.* **29**, 5976 (1984).

¹⁷Compare the discussion of short-ranged potentials in Ref. 6 and that of S. A. Trugman and S. Kivelson [*Phys. Rev. B* **31**, 5280 (1985)]. For a finite-size system the quasihole state (2.12) is not an exact eigenstate of the Hamiltonian in the limit of short-range interactions, because of problems associated with boundary excitations and center-of-mass motion; however, the state is exact for an infinite system, and Haldane's generalization is exact for a finite system on a sphere.

¹⁸Compare Ref. 4; also see T. Chakraborty and F. C. Zhang, *Phys. Rev. B* **29**, 7032 (1984); F. C. Zhang and T. Chakraborty, *ibid.* **30**, 7320 (1984).

¹⁹The definition of the proper quasiparticle energies $\tilde{\epsilon}_{\pm}$ given here coincide with the usage of Ref. 8 for the fundamental quantum Hall state, with $\nu = 1/m$. For higher-order states, such as $\nu = \frac{2}{5}, \frac{3}{7}$, etc., the quantities $\tilde{\epsilon}_{\pm}$ employed in Ref. 8

are not precisely the energy change resulting from the removal or addition of one flux quantum, but contain additional terms related to the hierarchical construction.

²⁰See, P. K. Lam and S. M. Girvin, *Phys. Rev. B* **30**, 473 (1984); **31**, 613(E) (1985).

²¹For a review, cf. K. Binder, in *Monte Carlo Method in Statistical Physics*, Vol. 36 of *Topics in Current Physics*, edited by K. Binder (Springer, New York, 1984).

²²Throughout this section the densities $\langle n(\mathbf{r}) \rangle$ apply to systems for which the change in the occupied area due to the presence of a quasiparticle or quasihole is not compensated.

²³For a review, see, for example, C. Domb, in *Phase Transitions and Critical Phenomena*, edited by C. Domb and M. S. Green (Academic, New York, 1974), Vol. 3, p. 42.

²⁴Chui *et al.* have employed a cumulant expansion to evaluate exchange contributions to the energy of their crystal-like wave function in Ref. 14. Although no details were presented, we believe that their method must be similar to the one employed here.

²⁵It is, in principle, conceivable that a trial wave function for the $\nu = \frac{2}{3}$ state might yield a lower value for the upper bound to the exact energy than the Laughlin $\nu = \frac{1}{3}$ hole wave function, thus providing also a better wave function for the $\nu = \frac{1}{3}$ electron state.

²⁶R. C. Tausworthe, *Math. Comput.* **19**, 201 (1965).

²⁷S. Kirkpatrick and E. P. Stoll, *J. Comput. Phys.* **40**, 517 (1981).